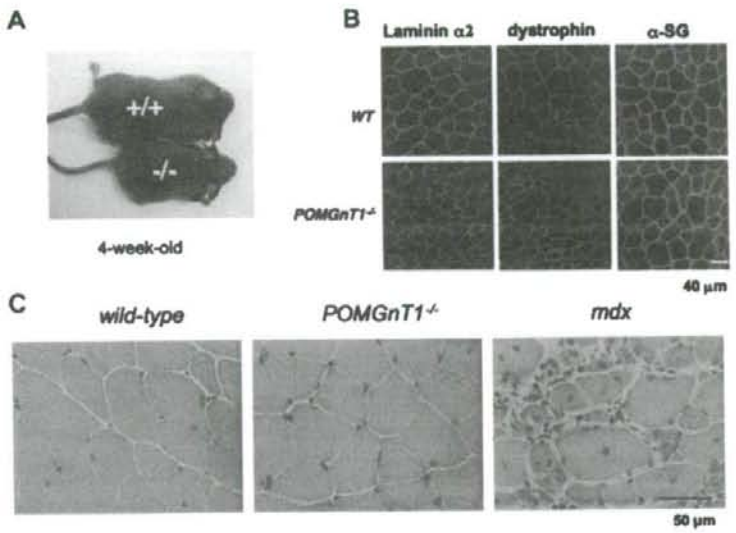

Fig. 3 – Remarkably mild dystrophic phenotypes of POMGnT1$^{-/-}$ muscle. (A) A photo of representative 4-week-old wild-type (+/+) and POMGnT1$^{-/-}$ (−/−) mice. POMGnT1$^{-/-}$ mice are smaller than wild-type littermates. (B) Immunohistochemistry of wild-type (+/+) and POMGnT1-knockout (−/−). Laminin α2 chain, dystrophin, and α-sarcoglycan are expressed normally on the sarcolemma of POMGnT1$^{-/-}$ muscle. (C) Representative H.E. staining of cross-sections of the TA muscles from POMGnT1$^{-/-}$, wild-type, and age-matched dystrophin-deficient *mdx* mice. POMGnT1$^{-/-}$ muscle shows minimal signs of degeneration and regeneration.

Table 1 – Summary of immunohistochemistry of hind-limb muscles of wild-type (WT) POMGnT1$^{-/-}$, and mdx mice.

	WT	POMGnT1$^{-/-}$	*mdx*
Laminin α2 chain	+	+	+
Dystrophin	+	+	−
α-Dystroglycan (VIA4-1)	+	−	±
Dystroglycan (core protein)	+	+	±
β-Dystropglycan	+	+	±
α-Sarcoglycan	+	+	±
α-Syntrophin	+	+	±
nNOS	+	+	±
Aquaporin 4	+	+	±
Integrin α7	+	+	++
Integrin β1	+	+	++

+, expressed; −, absent; ±, down-regulated; ++, up-regulated.

mice (Fig. 7). Three days after plating of single myofibers on Matrigel-coated 24-well plates in growth medium, the numbers of detached satellite cells (activated and proliferating satellite cells) were counted. In both extensor digitorum longus (EDL) (fast twitch muscle) and soleus (slow twitch muscle) muscles, the numbers of activated satellite cells and proliferating satellite cells (myoblasts) around the parental myofiber were more numerous in wild-type than in POMGnT1$^{-/-}$ (Fig. 7). Furthermore, wild-type satellite cells migrate a little faster than POMGnT1$^{-/-}$ satellite cells on transwells (data not shown), although the difference was little. Therefore, our results suggest that POMGnT1$^{-/-}$ satellite cells are activated more slowly or proliferate more slowly than wild-type. We next isolated satellite cells from hind limb muscles of wild-type and POMGnT1$^{-/-}$ mice by a monoclonal antibody, SM/C-2.6, and flow cytometry (Fukada et al., 2007), and examined their proliferation rate. The total yield of satellite cells per gram of POMGnT1$^{-/-}$ muscle tissue was nearly the same as those of wild-type muscle (data not shown). The percentage of Ki67-positive satellite cells (cycling cells) was less than 1% in both wild-type and POMGnT1$^{-/-}$ mice, indicating that they are in the quiescent stage (data not shown). However, after plating wild-type and POMGnT1$^{-/-}$ satellite cells onto Matrigel-coated 6-well plates at the same density, we found that POMGnT1$^{-/-}$ satellite cells grew poorly in growth medium (Fig. 7B). The timing of activation (i.e. enlargement of the cytoplasm and MyoD expression) was the same with that of wild-type satellite cells (data not shown). Next, we cultured satellite cells on Matrigel-coated 24-well-plates in growth medium, and the cells growth was evaluated by MTT assay 1, 2, 3, 4, 5, 6, and 7 days after plating (Fig. 8). The assay revealed that wild-type myoblasts proliferated more rapidly than POMGnT1$^{-/-}$ myoblasts *in vitro*. POMGnT1$^{-/-}$ myoblasts fused normally to form multinucleated myotubes in differentiation conditions like the wild-type (data not shown), and there was no significant difference in the fusion index between wild-type (45%) and POMGnT1$^{-/-}$ myoblasts (40%) ($p > 0.05$).

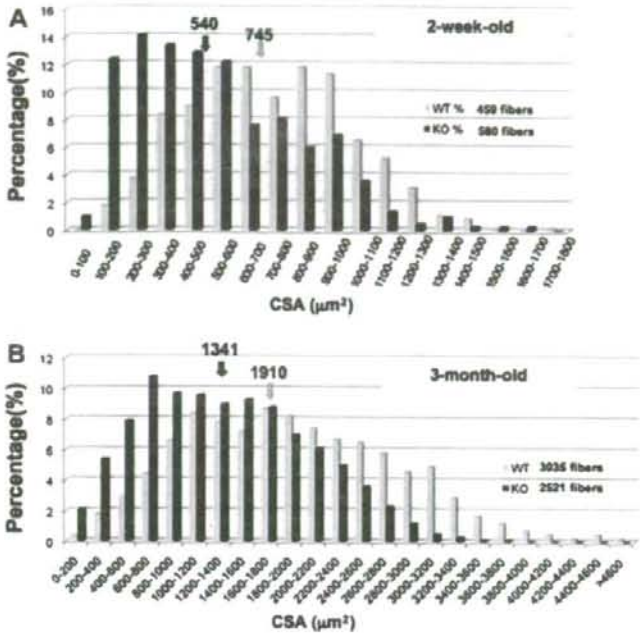

Fig. 4 – Cross-sectional area (CSA) of myofibers of POMGnT1$^{-/-}$ and wild-type mice. (A) A representative frequency graph of CSA of rectus femoris muscles from 2-week-old POMGnT1$^{-/-}$ (blue) and wild-type (light blue) littermates. The cross-sections were stained with anti-laminin α2 chain antibody. CSA of 459 POMGnT1$^{-/-}$ fibers and 580 wild-type fibers were measured and plotted. X-axis indicates CSA (μm²), and Y-axis indicates percentages. Arrows indicate the averages. The total number of myofibers was also reduced in POMGnT1$^{-/-}$ mice (4169 vs. 3510). (B) The CSA of myofibers in TA muscles from 3-month-old POMGnT1$^{-/-}$ (blue) and wild-type (light blue) male mice was plotted as in (A)). In (B), almost all myofibers were measured (3035 fibers in wild-type TA and 2521 fibers in POMGnT1$^{-/-}$ TA).

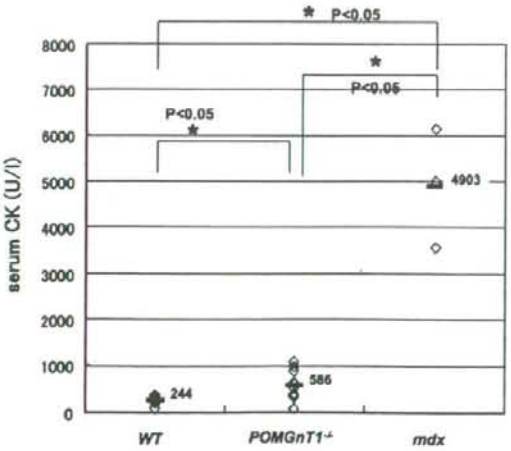

Fig. 5 – Serum CK levels of POMGnT1$^{-/-}$, wild-type, and *mdx* mice. Serum CK levels of 7–20 weeks old POMGnT1$^{-/-}$ mice (5 males and 5 females), wild-type littermates (3 males and 1 female), and three male *mdx* mice were measured and plotted on the graph with average. $^{*}p < 0.05$.

Next, we examined whether restoration of the expression of the POMGnT1 gene in mutant myoblasts improved their proliferation. To this end, we prepared a retrovirus vector, (pMX-POMGnT1-IRES-GFP) expressing human POMGnT1 and GFP. The recombinant retrovirus successfully restored O-mannosyl glycosylation of α-DG (Fig. 7A), but the proliferation rate was not changed (Fig. 8B).

2.5. *Cell growth signaling in POMGnT1$^{-/-}$ myoblasts*

It was previously reported that enhanced expression of α7β1 integrin ameliorates the development of muscular dystrophy and extends longevity in *α7BX2-mdx/utr*$^{(-/-)}$ transgenic mice (Burkin et al., 2001; Burkin et al., 2005), suggesting that integrin compensates for the function of α-DG in skeletal muscle to some extent. Therefore, we next examined the expression of β1-integrin in wild-type and POMGnT1$^{-/-}$ myoblasts (Supplementary Fig. 1). Western blotting, however, showed no difference between the β1-integrin protein levels in wild-type and POMGnT1$^{-/-}$ myoblasts (Supplementary Fig. 1A). Furthermore, FACS analysis showed similar levels of β1 integrin expression on the surfaces of myoblasts (Supplementary Fig. 1B). We then examined the activation levels of Akt and GSK-3β, both of which are involved in the

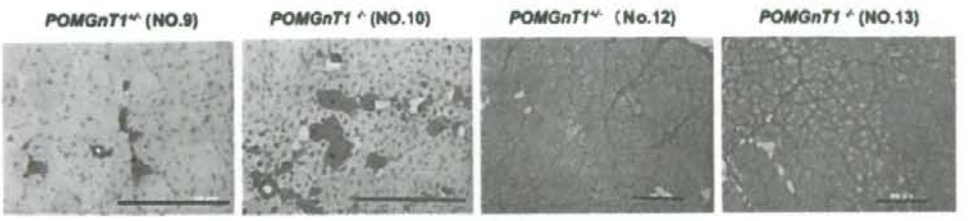

	genotype	sex	age	CTX interval (x3)	Fatty infiltration	Fibrosis
1	+/-	F	3M	2w	-	-
2	+/-	F	3M	2w	-	-
3	+/-	F	3M	2w	-→	-→
4	+/-	F	3M	2w	+	-→
5	-/-	M	3M	2w	+	-→
6	-/-	F	3M	2w	++	-→
7	+/-	F	11M	1w	+	+
8	-/-	F	8.5M	1w	+	++
9	+/-	F	8.5M	1w	+	-→
10	-/-	F	8.5M	1w	+→++	+→++
11	+/-	M	8.5M	1w	+	+
12	+/-	M	8.5M	1w	++	+
13	-/-	M	8.5M	1w	++	++

Fig. 6 – Impaired muscle regeneration of POMGnT1$^{-/-}$ mice. upper panel: representative Oil red O-stained or Sirius red-stained cross-sections of TA muscles of POMGnT1$^{-/-}$(−/−) and POMGnT1$^{+/-}$ (+/−) mice after three rounds of degeneration/regeneration evoked by cardiotoxin injection. One week after the last CTX injection, TA muscles were dissected, sectioned by a cryostat, fixed, and stained. lower table: Summary of fatty infiltration and fibrosis in regenerated muscles. CTX was injected into TA muscles three times with 2 weeks interval (2w) or 1 week interval (1w). The age at the first injection was shown. (–), well regenerated with minimal changes. (–→+), sporadic fatty regeneration or slight fibrosis between fibers. (+), mild fatty infiltration or mild fibrosis. (++), dense fatty infiltration or extensive fibrosis. F, female; M, male.

regulation of cell survival and proliferation. The levels of phosphorylation of these two kinases in POMGnT1$^{-/-}$ myoblasts were similar with those in wild-type myoblasts (Supplementary Fig. 1C). Consistent with these observations, TUNEL assay indicated that apoptosis is rare both in POMGnT1$^{-/-}$ and wild-type muscles (data not shown).

3. Discussion

In this study, we showed that in spite of mild muscle degeneration, the POMGnT1$^{-/-}$ satellite cells have much lower proliferative activity than wild-type satellite cells. The defect was not recovered by restoration of normal glycosylation of α-DG in mutant satellite cells. Together with the reduced sizes and the reduced numbers of myofibers of neonatal and adult POMGnT1$^{-/-}$ mice, these observations suggest that deficiency of POMGnT1 enzymatic activity impairs the functions of satellite cells.

3.1. *Two mouse models of muscle–eye–brain (MEB) disease*

Our POMGnT1$^{-/-}$ mice are the second mouse model of MEB disease. The first one was generated by gene trapping with a retroviral vector inserted into the second exon of the mouse POMGnT1 locus (Liu et al., 2006). As described in the literature, the phenotype is similar to ours with some differences. Our model shows much milder muscle phenotypes than the previously reported model, but also shows much a lower survival rate in the postnatal stage than the first model does. This would be due to more severe developmental abnormalities of the central nervous system of our mouse model, including disruption of the glia limitans, abnormal migration of neurons, and reactive gliosis in the cerebral cortex (manuscript in preparation), although these are also observed in the first model (Yang et al., 2007; Hu et al., 2007).

Mutation of the POMGnT1 gene is the cause of muscle–eye–brain disease (MEB) (Yoshida et al., 2001), which is characterized by severe congenital muscular dystrophy (Voit and Tome, 2004). Although glycosylation of α-DG was completely perturbed in our model, the POMGnT1$^{-/-}$ muscle showed only marginal pathological changes. Furthermore, POMGnT1$^{-/-}$ muscle showed normally formed muscle basal lamina on EM. These observations are in sharp contrast to the condition in humans. One possibility is that in the mouse, molecules other than α-DG are involved in the linkage of the sarcolemma with the extracellular matrix proteins, stabilizing the plasma membrane. As a candidate molecule, we examined β1-integrin expression in POMGnT1$^{-/-}$ muscle, but found that the level was not up-regulated. Therefore, the mechanism that explains this discrepancy remains to be clarified in a future study.

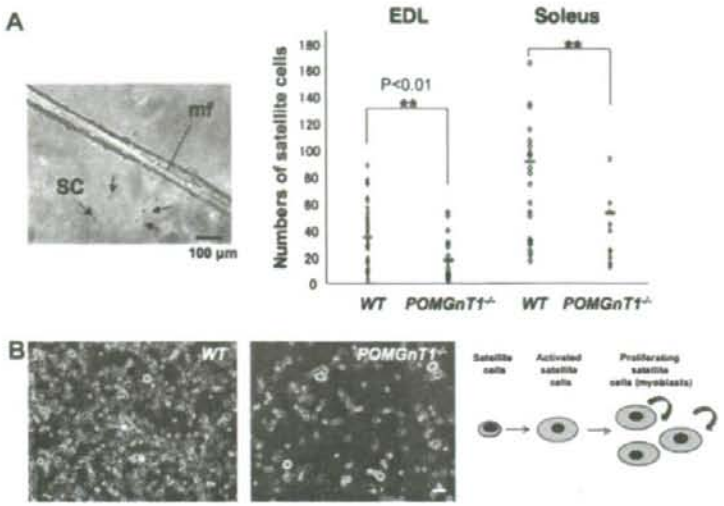

Fig. 7 – Activation and proliferation of satellite cells from WT and POMGnT1$^{-/-}$ mice. (A) Isolated myofibers were plated on Matrigel-coated 24 well-plates at one myofiber per well. Three days later, activated satellite cells (SC, arrows) around the parental fiber (mf) were counted and plotted. Small horizontal bars indicate the average number of activated/proliferating satellite cells originating from a myofiber from three independent experiments. Student's t-test. $^{**}p < 0.01$ (wild-type vs. POMGnT1$^{-/-}$ mice). (B) Satellite cells from WT and POMGnT1$^{-/-}$ mice 7 days after plating onto Matrigel-coated 24-well-plates at 2.5×10^3 cells/well. Scale bar, 100 μm.

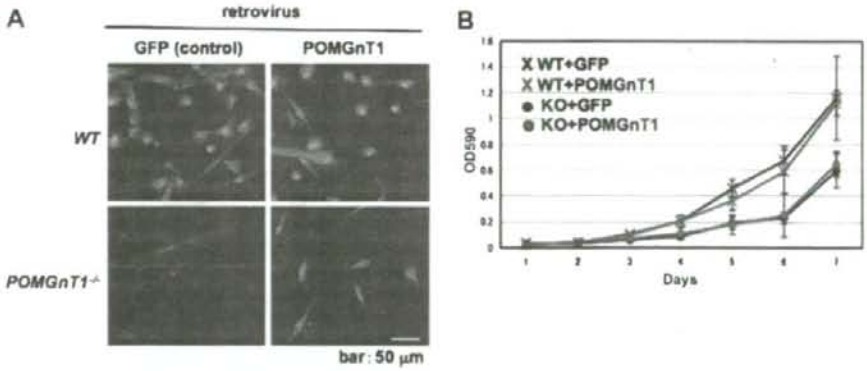

Fig. 8 – Restoration of POMGnT1 expression in POMGnT1$^{-/-}$ myoblasts does not improve proliferation of cells. (A) Wild-type (WT) and POMGnT1$^{-/-}$ myoblasts were transduced with a retrovirus expressing both POMGnT1 and GFP (POMGnT1) or only GFP (GFP, control), and the FACS-purified transduced cells were stained with anti-glycosylated α-DG monoclonal antibody (VIA4-1; red) and DAPI (Nucleus, blue). Note that the glycosylation of α-DG in POMGnT1$^{-/-}$ myoblasts was completely recovered by a retrovirus vector expressing POMGnT1. (B) MTT assay of wild-type (WT) and POMGnT1$^{-/-}$ myoblasts after infection with retrovirus vectors. Impaired proliferation of POMGnT1$^{-/-}$ myoblasts was not recovered by retrovirus-mediated expression of POMGnT1. Representative data of three independent experiments are shown.

3.2. *Null mutation in POMGnT1 reduces proliferative activity of muscle satellite cells*

POMGnT1$^{-/-}$ myoblasts proliferate poorly *in vitro*. This observation suggested that the proliferation of myoblasts is stimulated by growth signals *via* laminin-α-DG interaction. However, retrovirus vector-mediated gene transfer of the POMGnT1 gene, which successfully restored O-mannosyl glycosylation of α-DG, did not restore the proliferation activity of the POMGnT1$^{-/-}$ myoblasts. DMD myoblasts proliferate poorly and quickly reach senescence. The impaired proliferation activity has been ascribed to repeated activation of

satellite cells due to repetitive cycles of muscle degeneration and regeneration (Blau et al., 1983). In contrast, *POMGnT1*$^{-/-}$ muscle lacks signs of active regeneration. Therefore, the reduced proliferation activity of *POMGnT1*$^{-/-}$ mouse myoblasts is not likely due to excessive cell division of satellite cells. Rather, it is likely that α-DG-laminin interaction in the niche, i.e. beneath the basal lamina of skeletal muscle myofibers, is important for maintenance of proliferative activity of satellite cells. However, the possibility that POMGnT1-deficiency causes aberrant glycosylation of molecules other than α-DG should be also tested.

Our results also suggested that the lack of α-DG-laminin interaction resulted in reduced numbers of muscle fibers (hypoplasia). Importantly, we found that myofibers of older *POMGnT1*$^{-/-}$ mice tend to be hypertrophied (Supplementary Fig. 2). *POMGnT1*$^{-/-}$ muscle might compensate the muscle power by hypertrophy of the myofibers. This is consistent with our observation that *POMGnT1*$^{-/-}$ muscle increases its mass in an overload model (unpublished data). Importantly, recent studies suggest that this process is satellite cell-independent (Sandri M., 2008).

Recently, Liu et al. showed that over-expression of integrin α7β1 in C2C12 myoblasts promoted proliferation of the cells (Liu et al., 2008). Importantly, however, we did not observe up-regulation of integrin α7β1 expression in *POMGnT1*$^{-/-}$ satellite cells. These observations suggest that dystroglycans and integrins have distinct roles in the regulation of muscle satellite cells.

In summary, we generated *POMGnT1*-null mice. The mice showed low serum creatine kinase levels and minimal signs of muscle degeneration and regeneration. Nonetheless, *POMGnT1*$^{-/-}$ muscle showed the reduction in the size and the number of myofibers. Furthermore, repeated injection of cardiotoxin showed impaired muscle regeneration in *POMGnT1*$^{-/-}$ mice. *POMGnT1*$^{-/-}$ myoblasts proliferated poorly *in vitro*. Over-expression of protein restored glycosylation of α-DG, but did not improve the proliferation of *POMGnT1*$^{-/-}$ myoblasts at all. Collectively, our results suggest that POMGnT1 enzymatic activity is important for maintenance of the proliferative activity of satellite cells *in vivo*.

4. Experimental procedures

4.1. *Generation of POMGnT1*$^{-/-}$ *mice*

The targeting strategy in ES cells is depicted in Fig. 1. Genomic DNA (8.6 kb) covering almost the entire *POMGnT1* gene was isolated from 129/SvJ mice by using two specific primers: m1F2 primer, 5′-gat tcc tga agt cat gga ctg gc-3′ and m1B5, 5′-tct aaa ggt ctc tgt gtg agt ctg tca g-3′. The PCR product was then cloned into a TOPO TA cloning vector (Invitrogen, Carlsbad, CA) and sequenced (AB053221). To construct the targeting vector, a 630-bp RsrII-Hind III fragment, containing exon18 was replaced with a *neo* expression cassette (Stratagene) (Fig. 1). Electroporation and screening of ES cells (129Svev origin) were performed by Ingenious Targeting Laboratory, Inc. (Stony Brook, NY). Homologous recombination in ES cells was confirmed by Southern blotting. Two independent positive ES clones were injected into C57BL/6 blastocysts, which gave rise to offspring carrying the mutated allele. Genotyping of the mice was done by PCR. One primer set is designed to amplify exon 18: F2, 5′-cag cag ttt cct tcc ttc taa ccc-3′ and B4, 5′-att tgg tct ggt ccc ttg gct c-3′ (278 bp). *Neo* primers were used to amplify the *neo* resistance gene, and thereby detect the mutant allele: neo-F, 5′-agg cta ttc ggc tat gac tgg g-3′, and neo-R, 5′-tac ttt ctc ggc agg agc aag gtg-3′ (288 bp). Dystrophin-deficient *mdx* mice of C57BL/6 genetic background were provided by T. Sasaoka at the National Institute for Basic Biology, Japan. The Experimental Animal Care and Use Committee of the National Institute of Neuroscience approved all experimental protocols.

4.2. *POMGnT1 enzymatic activity*

Brains were obtained from 8-week-old mice and homogenized with nine volumes (weight/volume) of 10 mM Tris–HCl, pH 7.4, 1 mM EDTA, and 250 mM sucrose. After centrifugation at 900*g* for 10 min, the supernatant was subjected to ultracentrifugation at 100,000*g* for 1 h. The precipitates were used as the microsomal membrane fraction. The protein concentration was determined by BCA assay (Pierce, Rockford, IL). The enzymatic activity assay measured the amount of [^{3}H]GlcNAc transferred to a mannosyl peptide (Akasaka-Manya et al., 2004). Briefly, a reaction mixture containing 140 mM Mes buffer (pH 7.0), 1 mM UDP-[^{3}H]GlcNAc (80,000 dpm/nmol, PerkinElmer, Inc., Wellesley, MA), 2 mM mannosyl peptide (Ac-Ala-Ala-Pro-Thr-(Man)-Pro-Val-Ala-Ala-Pro-NH_2), 10 mM $MnCl_2$, 2% Triton X-100, 5 mM AMP, 200 mM GlcNAc, 10% glycerol, and 100 μg of microsomal membrane fraction was incubated at 37 °C for 1 h. After boiling for 3 min, the mixture was analyzed by reverse phase HPLC using a Wakopak 5C18-200 column (4.6 × 250 mm, Wako Pure Chemical Industries, Osaka, Japan). The gradient solvents were aqueous 0.1% trifluoroacetic acid (solvent A) and acetonitrile containing 0.1% trifluoroacetic acid (solvent B). The mobile phase consisted of 100% A for 10 min and then a linear gradient to 75% A:25% B over 25 min. Peptide separation was monitored at 214 nm, and the radioactivity of each fraction (1 ml) was measured using a liquid scintillation counter.

4.3. *Antibodies*

All antibodies used in Western blotting, immunohistochemistry, and FACS are listed in Supplementary Table 1.

4.4. *Histology and immunohistochemical analysis*

Muscle cryosections (6–10 μm) were stained with hematoxylin and eosin (H&E), or treated with 0.1% Triton X-100, blocked with 5% goat serum/1% BSA in PBS, then incubated with primary antibodies (Supplementary Table 1) at 4 °C overnight. After washing with PBS, specimens were incubated with a secondary antibody labeled with Alexa Fluor 488 or Alexa Fluor 568 (1:200–400 dilution; Molecular Probes) at RT for 1 h, counterstained with TOTO-3 (1:5000; Molecular Probes), and then mounted in Vectashield (Vector). The images were recorded using a confocal laser scanning microscope system TCSSP™ (Leica). For fiber size measurement, cross-sections of muscle were stained with anti-laminin α2

antibody and recorded and quantified by a digital microscope, BIOREVO (http://www.biorevo.jp; KEYENCE, Osaka, Japan).

4.5. Western blotting

Western blotting was performed as previously described (Hosaka et al., 2002). In brief, 20 μg of muscle proteins were separated on 7.5% SDS–PAGE gels and transferred to a PVDF membrane (Millipore, Bedford, MA). After incubation with primary antibodies (Supplementary Table 1), the membranes were incubated in HRP-labeled secondary antibodies (1:5000 dilution) (Amersham Biosciences, UK). The signals were detected by using an ECL plus Western Blotting Detection System (GE Healthcare, Buckinghamshire, UK).

4.6. Laminin blot overlay assay

An overlay assay was performed as described by Moore et al. (2002). In brief, WGA-enriched homogenates were prepared from wild-type and POMGnT1$^{-/-}$ brains, separated on SDS–PAGE gels, blotted onto a PDVF membrane, and incubated with mouse EHS laminin (Trevigen, Gaithersburg, MD, USA). Bound laminin was probed with anti-laminin antibody (Sigma, St. Louis, MO) and ECL system (GE Healthcare, Buckinghamshire, UK).

4.7. Single fiber preparation and culture

Single fibers were prepared from extensor digitorum longus (EDL) and soleus muscles of wild-type and POMGnT1$^{-/-}$ mice as described by Rosenblatt et al. (1995). Each fiber was plated onto Matrigel (BD Biosciences, Bedford, MA)-coated 24-well plates and cultured in growth medium for 3 days. Then, the number of cells around the parental fiber was counted.

4.8. Isolation of satellite cells, proliferation assay, and fusion index

Satellite cells were prepared from wild-type and POMGnT1$^{-/-}$ mice by FACS as previously described (Fukada et al., 2007). Sorted cells were plated on Matrigel-coated 24-well-plates at a density of 1×10^4 cells/well in a growth medium, DMEM (High glucose; Wako, Osaka), supplemented with 20% fetal bovine serum (Equitech-bio, Inc., Kerville, TX), human recombinant bFGF (2.5 ng/ml) (Invitrogen), recombinant mouse HGF (25 ng/ml) (R&D Systems, Minneapolis, MN), and heparin (5 μg/ml) (Sigma). For the MTT assay, 100 μl of 0.5% MTT (3-(4,5-dimethylthiazol-2-yl)-2,5-diphenyltetrazolium bromide) (Dojindo, Kumamoto, Japan) was added to the culture at each time point, and after 4 h incubation, the cells were collected in 1 ml of acid isopropanol solution. OD_{590} was measured and plotted. After reaching 70% confluency, the cells were induced to differentiate into myotubes by low-serum medium (5% horse serum/DMEM), and 18 h later, the cells were fixed, stained with anti-sarcomeric α-actinin antibody and DAPI (nuclei). Fusion index was calculated as (the numbers of nuclei in the myotubes/total nuclei) × 100%.

4.9. Production of retrovirus vectors

pMXs-IG (Kitamura et al., 2003) was kindly provided by T.Kitamura at Tokyo University. Human POMGnT1 cDNA, which has an Xpress epitope and a His-tag at the N-terminal (Akasaka-Manya et al., 2004), was cloned into the multi-cloning site upstream of IRES-GFP of the vector. Vector particles were produced by transfection of the vector plasmid into PLAT-E packaging cells (Kitamura et al., 2003). Proliferating satellite cells (myoblasts) were incubated with the viral vectors overnight and 4 days later, successfully transduced GFP-positive cells were collected by FACS, and the proliferation rate was evaluated by MTT assay.

4.10. Electron microscopy

Mice were perfused transcardially with a solution of 2% paraformaldehyde and 2.5% glutaraldehyde in PBS under deep pentobarbital anesthesia. The anterior tibial muscles were excised, embedded in 3% agarose, and sections (70 μm in thickness) were prepared on a Vibratome. Sections were fixed in OsO_4, ehydrated, and embedded in Cartepoxy resin. Ultrathin sections were prepared, stained with lead citrate and uranyl acetate, and observed under a Hitachi H-7000 transmission electron microscope.

4.11. Measurement of serum creatine kinase (CK)

Blood samples were obtained from the tail vein or directly from the heart at sacrifice. Serum CK level was measured by colorimetric assay using an FDC3500 clinical biochemistry autoanalyzer (FujiFilm Medical Co., Tokyo, Japan).

4.12. Cardiotoxin (CTX) injection

To induce muscle regeneration, CTX (10 μmol/L in saline; Sigma, St. Louis, MO) was injected into the tibialis anterior (TA) muscles three times at indicated intervals. The muscle cross-sections were stained with Oil red O (Muto Pure Chemicals Co., Ltd., Tokyo, Japan) to detect lipid droplets, or with Sirius red F3B (Sigma Chemical Co., St. Louis, MO) in saturated picric acid to stain collagen fibers.

Acknowledgments

This work was supported by Health Science Research Grants for Research on the Human Genome and Gene Therapy (H16-genome-003). For research on Phychiatric and Neurological Diseases and Mental Health (H18-kokoro-019; H20-016) from the Japanese Ministry of Health, Labor and Welfare, and Grants-in-Aid for Scientific Research (18590392) from the Japanese Ministry of Education, Culture, Sports, Science and Technology.

Appendix A. Supplementary data

Supplementary data associated with this article can be found, in the online version, at doi:10.1016/j.mod.2008.12.001.

REFERENCES

Akasaka-Manya, K., Manya, H., Kobayashi, K., Toda, T., Endo, T., 2004. Structure-function analysis of human protein O-linked mannose beta1,2-*N*-acetylglucosaminyltransferase 1, POMGnT1. Biochem. Biophys. Res. Commun. 320, 39–44.

Blau, H.M., Webster, C., Pavlath, G.K., 1983. Defective myoblasts identified in Duchenne muscular dystrophy. Proc. Natl. Acad. Sci. USA 80, 4856–4860.

Burkin, D.J., Wallace, G.Q., Milner, D.J., Chaney, E.J., Mulligan, J.A., Kaufman, S.J., 2005. Transgenic expression of α7β1 integrin maintains muscle integrity, increases regenerative capacity, promotes hypertrophy, and reduces cardiomyopathy in dystrophic mice. Am. J. Pathol. 166, 253–263.

Burkin, D.J., Wallace, G.Q., Nicol, K.J., Kaufman, D.J., Kaufman, S.J., 2001. Enhanced expression of the alpha 7 beta 1 integrin reduces muscular dystrophy and restores viability in dystrophic mice. J. Cell Biol. 152, 1207–1218.

Campanelli, J.T., Roberds, S.L., Campbell, K.P., Scheller, R.H., 1994. A role for dystrophin-associated glycoproteins and utrophin in agrin-induced AChR clustering. Cell 77, 663–674.

Cohn, R.D., Henry, M.D., Michele, D.E., Barresi, R., Saito, F., Moore, S.A., Flanagan, J.D., Skwarchuk, M.W., Robbins, M.E., Mendell, J.R., Williamson, R.A., Campbell, K.P., 2002. Disruption of DAG1 in differentiated skeletal muscle reveals a role for dystroglycan in muscle regeneration. Cell 110, 639–648.

Endo, T., Toda, T., 2003. Glycosylation in congenital muscular dystrophies. Biol. Pharm. Bull. 26, 1641–1647.

Fukada, S., Uezumi, A., Ikemoto, M., Masuda, S., Segawa, M., Tanimura, N., Yamamoto, H., Miyagoe-Suzuki, Y., Takeda, S., 2007. Molecular signature of quiescent satellite cells in adult skeletal muscle. Stem Cells 25, 2448–2459.

Gee, S.H., Montanaro, F., Lindenbaum, M.H., Carbonetto, S., 1994. Dystroglycan-alpha, a dystrophin-associated glycoprotein, is a functional agrin receptor. Cell 77, 675–686.

Hosaka, Y., Yokota, T., Miyagoe-Suzuki, Y., Yuasa, K., Imamura, M., Matsuda, R., Ikemoto, T., Kameya, S., Takeda, S., 2002. Alpha1-syntrophin-deficient skeletal muscle exhibits hypertrophy and aberrant formation of neuromuscular junctions during regeneration. J. Cell Biol. 158, 1097–1107.

Hu, H., Yang, Y., Eade, A., Xiong, Y., Qi, Y., 2007. Breaches of the pial basement membrane and disappearance of the glia limitans during development underlie the cortical lamination defect in the mouse model of muscle–eye–brain disease. J. Comp. Neurol. 502, 168–183.

Ibraghimov-Beskrovnaya, O., Ervasti, J.M., Leveille, C.J., Slaughter, C.A., Sernett, S.W., Campbell, K.P., 1992. Primary structure of dystrophin-associated glycoproteins linking dystrophin to the extracellular matrix. Nature 355, 696–702.

Kanagawa, M., Michele, D.E., Satz, J.S., Barresi, R., Kusano, H., Sasaki, T., Timpl, R., Henry, M.D., Campbell, K.P., 2005. Disruption of perlecan binding and matrix assembly by post-translational or genetic disruption of dystroglycan function. FEBS Lett. 579, 4792–4796.

Kanagawa, M., Toda, T., 2006. The genetic and molecular basis of muscular dystrophy: roles of cell–matrix linkage in the pathogenesis. J. Hum. Genet. 51, 915–926.

Kitamura, T., Koshino, Y., Shibata, F., Oki, T., Nakajima, H., Nosaka, T., Kumagai, H., 2003. Retrovirus-mediated gene transfer and expression cloning: powerful tools in functional genomics. Exp. Hematol. 31, 1007–1014.

Liu, J., Ball, S.L., Yang, Y., Mei, P., Zhang, L., Shi, H., Kaminski, H.J., Lemmon, V.P., Hu, H., 2006. A genetic model for muscle–eye–brain disease in mice lacking protein O-mannose 1,2-*N*-acetylglucosaminyltransferase (POMGnT1). Mech. Dev. 123, 228–240.

Liu, J., Burkin, D.J., Kaufman, S.J., 2008. Increasing alpha 7 beta 1-integrin promotes muscle cell proliferation, adhesion, and resistance to apoptosis without changing gene expression. Am. J. Physiol. Cell Physiol. 294, C627–C640.

Michele, D.E., Barresi, R., Kanagawa, M., Saito, F., Cohn, R.D., Satz, J.S., Dollar, J., Nishino, I., Kelley, R.I., Somer, H., Straub, V., Mathews, K.D., Moore, S.A., Campbell, K.P., 2002. Post-translational disruption of dystroglycan–ligand interactions in congenital muscular dystrophies. Nature 418, 417–422.

Moore, S.A., Saito, F., Chen, J., Michele, D.E., Henry, M.D., Messing, A., Cohn, R.D., Ross-Barta, S.E., Westra, S., Williamson, R.A., Hoshi, T., Campbell, K.P., 2002. Deletion of brain dystroglycan recapitulates aspects of congenital muscular dystrophy. Nature 418, 422–425.

Peng, H.B., Ali, A.A., Daggett, D.F., Rauvala, H., Hassell, J.R., Smalheiser, N.R., 1998. The relationship between perlecan and dystroglycan and its implication in the formation of the neuromuscular junction. Cell Adhes. Commun. 5, 475–89.

Rosenblatt, J.D., Lunt, A.I., Parry, D.J., Partridge, T.A., 1995. Culturing satellite cells from living single muscle fiber explants. In Vitro Cell Dev. Biol. Anim. 31, 773–779.

Sandri M., 2008. Signaling in muscle atrophy and hypertrophy. Physiology (Bethesda) 23, 160–170.

Sugita, S., Saito, F., Tang, J., Satz, J., Campbell, K., Südhof, T.C., 2001. A stoichiometric complex of neurexins and dystroglycan in brain. J. Cell Biol. 154, 435–445.

Voit, T., Tome, F.S., 2004. The congenital muscular dystrophies. In: Engel, A.G., Franzini-Armstrong, C. (Eds.), Myology. McGraw-Hill, New York, pp. 1203–1238.

Yang, Y., Zhang, P., Xiong, Y., Li, X., Qi, Y., Hu, H., 2007. Ectopia of meningeal fibroblasts and reactive gliosis in the cerebral cortex of the mouse model of muscle–eye–brain disease. J. Comp. Neurol. 505, 459–477.

Yoshida, A., Kobayashi, K., Manya, H., Taniguchi, K., Kano, H., Mizuno, M., Inazu, T., Mitsuhashi, H., Takahashi, S., Takeuchi, M., Herrmann, R., Straub, V., Talim, B., Voit, T., Topaloglu, H., Toda, T., Endo, T., 2001. Muscular dystrophy and neuronal migration disorder caused by mutations in a glycosyltransferase, POMGnT1. Dev. Cell 1, 717–724.

A Renaissance for Antisense Oligonucleotide Drugs in Neurology

Exon Skipping Breaks New Ground

Toshifumi Yokota, PhD; Shin'ichi Takeda, MD, PhD; Qi-Long Lu, MD, PhD; Terence A. Partridge, PhD; Akinori Nakamura, MD, PhD; Eric P. Hoffman, PhD

Antisense oligonucleotides are short nucleic acid sequences designed for use as small-molecule drugs. They recognize and bind to specific messenger RNA (mRNA) or pre-mRNA sequences to create small double-stranded regions of the target mRNA that alter mRNA splicing patterns or inhibit protein translation. Antisense approaches have been actively pursued as a form of molecular medicine for more than 20 years, but only one has been translated to a marketed drug (intraocular human immunodeficiency virus treatment). Two recent advances foreshadow a change in clinical applications of antisense strategies. First is the development of synthetic DNA analogues that show outstanding stability and sequence specificity yet little or no binding to modulator proteins. Second is the publication of impressive preclinical and clinical data using antisense in an exon-skipping strategy to increase dystrophin production in Duchenne muscular dystrophy. As long-standing barriers are successfully circumvented, attention turns toward scale-up of production, long-term toxicity studies, and the challenges to traditional drug regulatory attitudes presented by tightly targeted sequence-specific drugs.

Arch Neurol. 2009;66(1):32-38

With the advent of recombinant DNA in the 1970s, it was soon realized that bacteria possess a form of regulatory machinery where small RNA transcripts can bind (hybridize) to other target RNAs and inhibit the translation of these targets.[1] These antisense RNAs were subsequently recognized as natural translational regulation mechanisms in plants and higher organisms.[2] More recently, a specialized form of antisense transcript was found to be a cellular defense mechanism against invading messenger RNAs (mRNAs) (viruses), and this has been harnessed as a popular method to "knock down" specific mRNA transcripts in cultured cell models (short interfering RNAs).[3]

Attention soon shifted toward development of antisense molecules as a form of small-molecule drug (antisense oligonucleotide [AO]). The approach was intuitive: one needs simply to chemically synthesize short pieces of DNA of about 20 bases, where a specific complementary sequence is designed to hybridize with a desired target mRNA. Such designer AO drugs should show very high specificity and selectivity for binding only the desired target RNA sequence of nucleotides that is predicted by base pairing. Beginning in the mid-1980s, this approach was put to the test in model systems and was shown to work quite well in shutting down the production of the target (undesired) protein.[4] Isis Pharmaceuticals, Inc, Carlsbad, California, a company focused on clinical applications of AOs, was incorporated in 1989. Additional companies focusing on AO approaches soon followed.

Despite early promise, uses of AOs as small-molecule drugs have been painfully slow to enter the market and standard of care. Indeed, only a single AO drug has been approved by the Food and Drug

Author Affiliations: Research Center for Genetic Medicine, Children's National Medical Center, Washington, DC (Drs Yokota, Partridge, and Hoffman); Department of Molecular Medicine, National Institutes for Neuroscience, Tokyo, Japan (Drs Takeda and Nakamura); and McColl-Lockwood Laboratory for Muscular Dystrophy Research, Neuromuscular/ALS Center, Carolinas Medical Center, Charlotte, North Carolina (Dr Lu).

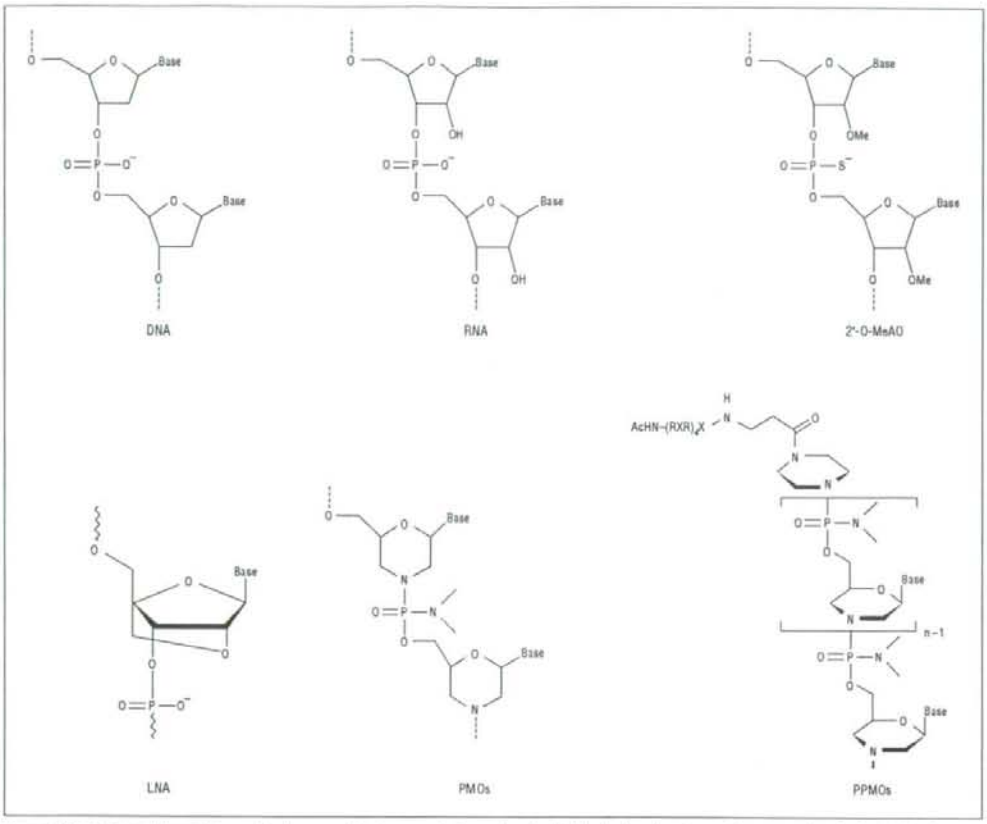

Figure 1. Comparison of chemistries used for the exon-skipping approach. Examples of artificially developed antisense oligomers such as 2′-O-methylated antisense oligonucleotides (2′-O-MeAO) (phosphorothioate), locked nucleic acid (LNA), phosphorodiamidate morpholino oligomers (PMOs), and peptide-tagged PMOs (PPMOs) are shown for comparison with DNA and RNA.

Administration (FDA), fomivirsen sodium (Vitravene; Isis Pharmaceuticals, Inc) delivered by intravitreous injection to inhibit cytomegalovirus retinitis in AIDS. Vitravene was approved in 1998 and there have been no subsequent successful approvals in the ensuing 10 years.

What has slowed the progress of AO drugs into the clinical arena, and why may this be changing?

There have been 2 major hurdles: off-target toxic effects and potency or delivery. Regarding toxic effects, most organisms do not take kindly to covert infiltration by foreign DNA or RNA. Indeed, all species have quite effective mechanisms to destroy foreign DNA and RNA as they are more likely than not to be viruses or other undesirable organisms. In addition, many of the clinical trials testing AO drugs have seen evidence of activation of the complement cascade, and this has been a key concern of the FDA. Delivery has also been a consistent problem. Because the target RNAs are always intracellular, it is imperative for the AO drug to achieve intracellular concentrations sufficient to enable it to bind and modulate the target RNA to a significant extent. The fact that AOs typically do not easily cross the lipid bilayers that bound the cell so as to achieve sufficient intracellular potency via systemic (intravenous) delivery has been problematic.

Recent developments are achieving success in overcoming both hurdles. Analogues of nucleic acid have been designed and synthesized in which the ribose backbone of RNA and DNA is replaced with different chemistries (**Figure 1**). Two are particularly promising: one uses a morpholino backbone (phosphorodiamidate morpholino oligomer [PMO]; AVI BioPharma, Portland, Oregon), and the second uses a locked nucleic acid backbone (Enzon Pharmaceuticals, Inc, Bridgewater, New Jersey). These new backbones are designed to maintain the molecular distance between bases (G, A, T/U, and C), enabling highly sequence-specific base pairing to the target RNA that is stronger in the case of PMO and locked nucleic acid drugs than DNA or RNA AOs. Equally important, these backbones are so dissimilar from the DNA and RNA ribose phosphodiester backbone that they are not recognized by most or any DNA and RNA binding proteins or degrading enzymes, thereby enhancing their stability and avoiding many or all off-target toxic effects.

The second major barrier has been achieving sufficient intracellular concentrations (delivery). One successful approach is to take advantage of preexisting holes in the plasma membrane of the target cell. Infecting viruses breach the cell membrane during the process of infection and appear to bring along AO drugs in the process. As such, AOs have been quite successful in blocking downstream viral replication within cells, and PMO drugs are showing impressive promise as antiviral antidotes.[5] Another preexisting hole is found in muscle cells lacking dystrophin (Duchenne muscular dystrophy [DMD]).[6] The unstable plasma membrane of myofibers appears to allow the AO to leak into the cell.[7] An additional approach is to modify the AO drugs with cell delivery moieties, chemical adducts that penetrate the cell membrane. One example is the addition of arginine-rich peptides to one end of the AO drug (peptide-tagged PMO) (Figure 1).

From these advances has sprung a resurgence of interest in AO drugs for treatment of genetic disease, cancer, and infectious disease. The purpose of most applications is to knock down a target RNA so that it makes less of the deleterious protein product (eg, tumor growth factor β or hypoxia-inducible factor 1α in cancer cells, viral mRNAs, or dominant gain-of-function toxic proteins in inherited neurological disease). However, the disorder that may be most advanced in such applications is DMD. Here the AOs are used for a quite different objective than for previous applications; explicitly, AOs in DMD are designed to restore function to the target mRNA and protein rather than block it. The remainder of this review focuses on this application.

RATIONALE AND PROOF OF PRINCIPLE OF EXON-SKIPPING THERAPY

The principle of exon-skipping therapy for dystrophinopathies was initially demonstrated by Dunckley et al[8] in cultured mouse muscle cells in vitro. The rationale is as follows. Duchenne muscular dystrophy is caused by mutations of the 79-exon gene (commonly deletions of ≥1 exon). Within the myofiber, the remainder of the gene will be transcribed and spliced together. However, if the triplet codon reading frame of the mRNA is not preserved, the resulting frame shift will lead to the failure of dystrophin protein production. Becker muscular dystrophy (BMD) is a clinically milder and more variable disease in which mutations of the dystrophin gene are commonly such as to preserve the translational open reading frame; thus, after splicing together, the remainder of the gene retains some ability to synthesize the dystrophin protein. The goal of exon-skipping therapies is to force the dysfunctional mRNA with out-of-frame mutations in a patient with DMD to skip (exclude) some additional exons. The loss of additional material directed by AO drugs restores the reading frame, changing a Duchenne out-of-frame transcript to a Becker in-frame transcript. Fortunately, most mutations in the dystrophin gene occur in parts that do not code for functionally essential regions of the protein.

This AO-mediated exon-skipping method has been developed and extensively tested on the dystrophic *mdx* mouse model of DMD. The *mdx* mouse harbors a nonsense mutation in exon 23 that prevents translation beyond this point in the transcript. Both local intramuscular injection and systemic delivery of a single AO targeted against exon 23 in the primary transcript excludes this exon from the mRNA, leaving an in-frame transcript that generates dystrophin expression and produces a degree of functional recovery. Intramuscular and systemic injections of AOs for exon splicing of a dog model of DMD have also been demonstrated with a novel cocktail AO strategy (T.Y., S.T., Q.-L.L., T.A.P., A.N., E.P.H., and Masanori Kobayashi, DVM, unpublished data, 2006-2008). The principle is similarly illustrated in humans; van Deutekom et al[9] reported single-site intramuscular injections of 2′-O-methyl AO chemistry in 4 boys with DMD, showing evidence of de novo dystrophin production at the injection site.

These data demonstrate that the key hurdles of achieving intracellular delivery and avoiding toxic effects can be cleared. A similar strategy is being explored in other diseases such as myotonia, human immunodeficiency virus, and spinal muscular atrophy.[10-12]

HURDLES IN BRINGING EXON SKIPPING TO STANDARD OF CARE

Exon skipping using AO drugs has rapidly emerged as the frontline therapeutic approach for DMD. How soon can we expect exon skipping to reach the neuromuscular clinic and standard of care? This approach is breaking new ground and raising challenges not encountered previously in drug development. Different patients have different mutations, and many AO sequences will need to be designed, tested, and FDA approved. Also, current genotype and phenotype data suggest that there may be good in-frame deletions and not-so-good in-frame deletions; simply restoring the reading frame may not be synonymous with restoring dystrophin protein function. The optimization of dystrophin function will likely require deletions of multiple exons, and this will require mixtures of different AOs—new territory for drug development and the FDA. The approach will require regular injections of large amounts of AO drug; what are the long-term toxic effects? Moreover, are the standard toxicity tests appropriate for sequence-specific drugs? Each of these hurdles is discussed briefly in the remainder of this review.

CERTAIN EXON DELETIONS MAY RETAIN MORE DYSTROPHIN FUNCTION THAN OTHERS

The molecular diagnostics of DMD and BMD frequently refer to the reading frame rule, where out-of-frame deletions are given a DMD diagnosis and in-frame deletions are given a BMD diagnosis. However, as many as 30% of patients with BMD do not adhere to this rule.[13] A thorough understanding of reading frames is critical for appropriate design of exon-skipping therapies, both so that the best AO can be given to the patient and so that an optimally functional dystrophin protein is produced as a result of the expected exon skipping. Currently, the best information from which to predict the capabilities of partially deleted dystrophins to rescue the DMD phenotype comes from analysis of the thousands of geno-

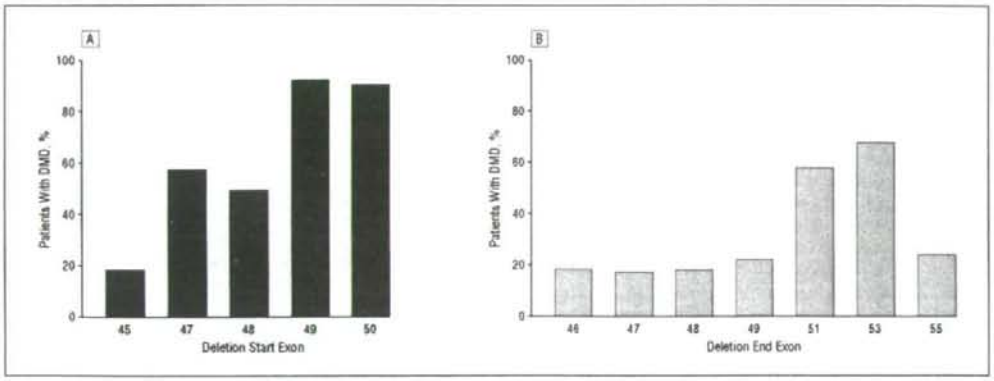

Figure 2. Clinical phenotypes associated with specific start (A) and end (B) sites for in-frame deletions. Percentages of patients with Duchenne muscular dystrophy (DMD) out of patients with DMD or Becker muscular dystrophy with specific start and end exons are shown. Combined muscular dystrophy databases of 14 countries (from Argentina, Belgium, Brazil, Bulgaria, Canada, China, Denmark, France, India, Italy, Japan, The Netherlands, the United Kingdom, and the United States) at Leiden University (http://www.dmd.nl), where diagnoses were performed using multiplex ligation-dependent probe amplification/multiplex amplification and probe hybridization, Southern blotting, or polymerase chain reaction primer sets that allow deletion boundaries to be assigned accurately to a specific exon, are used (deletion start sites: n=288 for exon 45, n=23 for exon 47, n=9 for exon 48, n=12 for exon 49, and n=10 for exon 50; deletion end sites: n=11 for exon 46, n=115 for exon 47, n=95 for exon 48, n=51 for exon 49, n=53 for exon 51, n=40 for exon 53, and n=21 for exon 55).

type and phenotype correlations in patients with DMD and BMD that have been published in the literature and on the Internet. We examined all in-frame deletions and determined the proportion of observed cases that showed mild or severe phenotypes. This was gleaned from combined muscular dystrophy databases of 14 countries (from Argentina, Belgium, Brazil, Bulgaria, Canada, China, Denmark, France, India, Italy, Japan, The Netherlands, the United Kingdom, and the United States) at Leiden University (http://www.dmd.nl), excluding diagnoses that did not allow deletion boundaries to be assigned accurately to a specific exon.[14] Of all observed in-frame deletion patterns on genomic DNA in the central rod domain hotspot region (exons 42-57; 28 distinct patterns), 57% (16 of 28 patterns) were associated with DMD rather than BMD. This analysis showed that there are considerable discrepancies between population-based ratios and pattern-based proportions of severe DMD vs mild BMD phenotypes, and interestingly, the ratio of DMD to BMD remarkably varies between specific deletion patterns. For example, in-frame deletions starting or ending around exon 50 or 51 that encode the hinge region were most commonly associated with severe phenotypes (**Figure 2**) (eg, deletions at exons 47-51, 48-51, and 49-53 are all reported to be associated with a severe DMD phenotype rather than BMD).[15,16]

Two questions arise. First, why do specific patterns of in-frame mutations tend to result in a severe DMD phenotype in contradiction to the reading frame rule? Second, why do different individuals with the same exonic deletion pattern exhibit such different clinical phenotypes? Likely contributory factors include the following: the effect of the specific deletion breakpoints on mRNA splicing efficiency and/or patterns; translation or transcription efficiency after genome rearrangement; and stability or function of the truncated protein structure. The mechanisms controlling accurate splicing of the 79-exon, 2.4 million–base pair dystrophin gene are clearly complex. Introns of the dystrophin gene are highly variable in size, and it is likely that exonic splicing does not take place in an ordered 5′ to 3′ sequence. A complication in interpreting genotype and phenotype correlations is that the deletion in genomic DNA does not always correspond to the material missing from the resulting mRNA. We and others have shown that even in the absence of AOs, a patient may produce 1 or more transcripts that skip additional exons present in the genomic DNA, in effect performing their own private exon skipping.[13] Disruption of splice site information (such as an intervening sequence) in some patients with in-frame gene deletions may cause skipping of additional exons at mRNA splicing, thus leading to out-of-frame transcripts from an in-frame genomic DNA deletion as Kesari et al[13] have recently described. As Menhart[17] has pointed out, it is also likely that quasi-dystrophin variants in the rod domain may show different stability or function because of different types of derangement of spectrinlike repeat domains. Not enough is known about dystrophin structure and function, and the relative importance of the protein sequence within the rod domain remains entirely a matter of speculation. Historically, lack of dystrophin expression has been used as the key criterion for DMD diagnosis. This together with the presence of the DMD clinical picture with such in-frame mutations argues that other confounding variables such as imprecisely defined mutation or aberrant splicing may explain these "exceptions to the reading frame rule." Thus, it is anticipated that most or all patients with mutations in the central rod domain would benefit from the production of truncated dystrophin.

PARALLELING AO TRIALS: TESTING NEW EXONS AND MIXTURES

Clinical proof-of-concept trials testing limited intramuscular injection with a 2′-O-methyl AO against exon 51

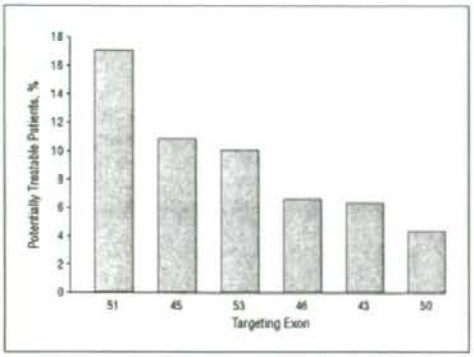

Figure 3. Targets of exon skipping and population of potentially treatable patients. Percentage of patients with the dystrophin deletion who are potentially treatable by targeting specific exons for Duchenne muscular dystrophy. For example, 17% of patients with Duchenne muscular dystrophy who have the dystrophin deletion can be potentially treated by targeting exon 51 using antisense oligonucleotides.

have been published,[9] and similar studies with PMO chemistry are under way in the United Kingdom. Given the many questions concerning the sequence specificity of toxic effects and the large number of AO sequences that will need to be developed as drugs to treat most patients with DMD, it is critical to parallel studies on many more AOs for DMD (**Figure 3**).

It should be noted that about 30% of patients with DMD have nondeletion mutations (duplication, nonsense mutations, small rearrangement, or splice site mutations). Most mutations are theoretically amenable to exon skipping; however, there are no hot spots for point mutations, so relatively few patients would be treatable with each targeted exon by comparison with deletion mutations. Moreover, if skipped to remove a nonsense mutation, the exons that are candidates to restore the reading frame in patients with deletions (eg, exons 43, 45, 46, 50, 51, and 53) will require additional deletion of at least 1 further exon to restore the reading frame because these are frame-shifting exons. Thus, only 35% of nonsense mutations are potentially treatable by single-exon targeting, but the combined data of the Leiden DMD mutation database imply that more than 90% could be responsive to multiskipping.[14]

Development of exonic cocktails (mixtures) could resolve a number of problems, including optimization of dystrophin function and covering relatively high proportions of patients with DMD with a single mixture. The mixture approach has clear advantages and disadvantages. As an example, an 11-exon AO cocktail skipping exons 45 through 55 is predicted to result in a particularly mild BMD phenotype (94% of reported patients).[14] Encouragingly, this large deletion is regularly associated with clinically milder phenotypes than any of the smaller in-frame deletions within the same range of exons 45 to 55.[18] A second advantage is that the cocktail could conceivably be approved as a single drug for most patients with DMD who have dystrophin deletions, independent of their precise deletion, eg, an 11-exon AO cocktail targeting exons 45 through 55 is potentially applicable to more than 60% of patients with a dystrophin deletion (**Figure 4**).[18,19] In total, more than 90% of patients with DMD could potentially be treated by multiskipping, whereas single-exon skipping could treat around half of the patients with dystrophin deletions and point mutations. Systemic studies in the large dog model of DMD have been done using a 3-exon PMO cocktail, and this has clearly been shown to be efficacious by multiple clinical, imaging, histological, and biochemical or molecular end points (T.Y., S.T., Q.-L.L., T.A.P., A.N., E.P.H., and Masanori Kobayashi, DVM, unpublished data, 2006-2008).

A disadvantage of the cocktail approach is the addition of novel hurdles for FDA or regulatory approval. Current FDA regulations require each component of a drug mixture to undergo toxicological and clinical testing and then require the mixture to similarly undergo toxicological and clinical testing. In the context of an ideal 11-exon AO cocktail, the regulatory barriers become truly intimidating. In addition, the 11-exon cocktail PMO approach would lead to delivery of some AOs that may not have a target in a specific patient (eg, the patient already has a deletion of ≥1 exon in the AO mix). Thus, some parts of the mixture will have no possible potential molecular or clinical benefit to individual patients. This would again be uncharted territory for the FDA. While clinical development of the 11-exon mixture is likely ambitious at present, it will be important to initiate toxicological and clinical trials of exon mixtures for subsets of patients who cannot be treated with a single AO. Also, for future trials on multiskipping such as with exons 45 through 55, we should have as many AOs in hand as possible because they can be used as part of multiskipping AOs.

PERSONALIZED MEDICINE AND THE FDA: ARE EXISTING GUIDELINES APPROPRIATE?

Personalized medicine has many definitions, but most share the concept of optimizing a treatment for a particular patient. Designing and using AO drugs targeted for a patient's specific gene mutation would seem to fit well within this rubric. As such, the promising AO exon-skipping approach may bring neuromuscular disease to the frontline in development of drugs for personalized medicine. It is important to examine the existing FDA guidelines for drug development and reinterpret these guidelines in the context of AO and DMD. For example, the drug development pipeline includes phase 1 studies of the drug in healthy volunteers. However, successful on-target exon skipping of the dystrophin gene in healthy volunteers would give them DMD, a clear adverse effect that is entirely irrelevant to toxic effects in the target patient population (boys with DMD). Toxicity tests are currently done in animal models (typically 2 species), but one of the major concerns regarding toxic effects of AO drugs is binding to off-target RNAs. For example, if an AO drug designed for exon skipping of the dystrophin mRNA also binds to the closely related utrophin mRNA, then exon skipping of utrophin might occur and could result in off-target adverse effects. The utrophin sequence of mice or rats is different from the utrophin sequence of humans, so the standard rodent toxicity tests

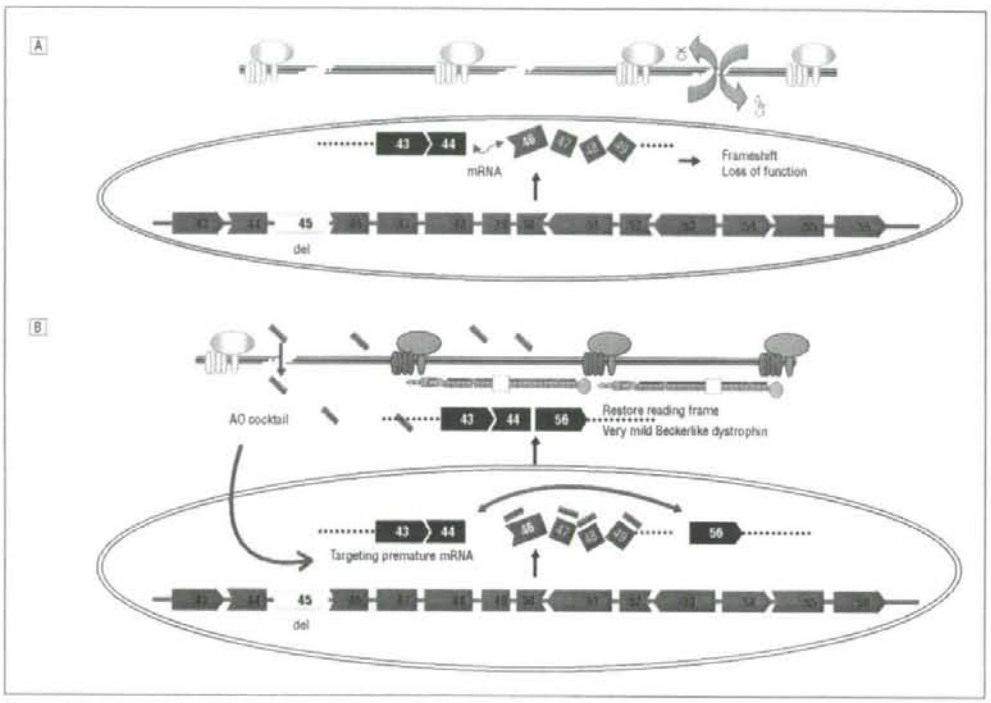

Figure 4. Mechanism of multiexon skipping of exons 45 through 55 to rescue 60% of patients with Duchenne muscular dystrophy with dystrophin deletions. A, More than 60% of deletion mutations of the dystrophin gene occur within the hot-spot range of exons 45 through 55 (exon 45 is deleted in this schematic [del]) in Duchenne muscular dystrophy muscles. The messenger RNA (mRNA) of remaining exons is spliced together but the reading frame is disrupted, resulting in failure of the production of functional dystrophin protein. CK indicates creatine kinase; Ca^{2+}, calcium ions. B, An antisense oligonucleotide (AO) cocktail targeting exons 45 through 55 likely enters the Duchenne muscular dystrophy muscle through its leaky membranes, then binds to the dystrophin mRNA in a sequence-specific manner. The AOs block the splicing machinery and prevent inclusion of all exons between exons 45 and 55. Skipping these exons restores the reading frame of mRNA, allowing production of quasi-dystrophin containing exons 1 through 44 and exons 56 through 79, which is not normal but likely retains considerable function as evidenced by patients with clinically milder Becker muscular dystrophy with identical partial dystrophin.

may not accurately assess off-target toxic effects of AOs for human use.

Perhaps the largest challenge facing implementation of exon-skipping therapy for DMD is in developing new approaches to toxicity testing and clinical trial regulatory procedures that are relevant and appropriate for sequence-specific drugs. The pharmaceutical industry often quotes a price tag of $500 million to bring any new drug to the market. Given the discussion earlier, implementation of AO drugs in DMD will require many exon-specific drugs. If the $500 million is assessed for each individual AO sequence, then both time and money become insuperable barriers to helping the existing generation of boys with DMD. The silver lining in this cloud is the lack of any detectable toxic effects with PMO AO drugs to date. If multiple AOs all show a lack of long-term toxic effects, then there is hope that specific AO drugs could be approved with more limited toxicological and phase 1 testing.

A practical resolution of this problem is to consider each component of the potential toxic effects of these highly targeted drugs individually. Tests of the generic toxic effects of morpholinos at the doses at which they are likely to be functionally effective could be conducted quite straightforwardly with either a scrambled or arbitrary sequence of a particular molecular weight. It is the notion of individual sequence-specific toxic effects that raises problems. The argument that any specific sequence may have off-target effects (eg, binding to utrophin transcripts) cannot be properly tested in other species because they may have different potential off-target sequences as compared with those in humans. This carries the dire implication that a lack of sequence-specific toxic effects in a test species can provide no assurance, indeed no information at all, as to the sequence's safety in humans. Tests in healthy human volunteers are also problematic. Ethical issues arise from the possible generation of a pathogenic frameshift in healthy muscle by successful suppression of the targeted exon. Moreover, the lack of innate pathological abnormalities in healthy human muscle would stifle access of the AO to its intended intramuscular target while at the same time providing a different spectrum of potential off-target molecules (eg, utrophin transcripts). A further complication arises from the individualistic nature of the entire rationale, for it precludes the possibil-

ity of learning from experience; the probability that any given sequence may be toxic is independent of the number of safe experiences with other sequences. In effect, for safety, we can test for sequence-specific toxic effects only in human volunteers with DMD by progressive dose escalation. Only in this way would the reagents have access to their intended targets as well as any unintended targets in a physiological context that is inappropriately modeled both in other species and in healthy human volunteers.

Accepted for Publication: April 15, 2008.
Correspondence: Eric P. Hoffman, PhD, Research Center for Genetic Medicine, Children's National Medical Center, 111 Michigan Ave NW, Washington, DC 20010 (ehoffman@cnmcresearch.org).
Author Contributions: *Study concept and design:* Yokota, Takeda, Partridge, and Hoffman. *Acquisition of data:* Yokota and Lu. *Analysis and interpretation of data:* Yokota, Nakamura, and Hoffman. *Drafting of the manuscript:* Yokota, Partridge, Nakamura, and Hoffman. *Critical revision of the manuscript for important intellectual content:* Takeda, Lu, and Partridge. *Obtained funding:* Hoffman. *Administrative, technical, and material support:* Lu. *Study supervision:* Yokota, Takeda, Partridge, Nakamura, and Hoffman.
Financial Disclosure: None reported.
Funding/Support: This work was supported by the Foundation to Eradicate Duchenne, Jane Foundation, the Muscular Dystrophy Association, and a collaborative grant from the National Institutes of Health Wellstone Muscular Dystrophy Research Centers (http://www.wellstone-dc.org).

REFERENCES

1. Spiegelman WG, Reichardt LF, Yaniv M, Heinemann SF, Kaiser AD, Eisen H. Bidirectional transcription and the regulation of phage lambda repressor synthesis. *Proc Natl Acad Sci U S A*. 1972;69(11):3156-3160.
2. Kumar M, Carmichael GG. Antisense RNA: function and fate of duplex RNA in cells of higher eukaryotes. *Microbiol Mol Biol Rev*. 1998;62(4):1415-1434.
3. Gitlin L, Karelsky S, Andino R. Short interfering RNA confers intracellular antiviral immunity in human cells. *Nature*. 2002;418(6896):430-434.
4. Kim SK, Wold BJ. Stable reduction of thymidine kinase activity in cells expressing high levels of anti-sense RNA. *Cell*. 1985;42(1):129-138.
5. Warfield KL, Swenson DL, Olinger GG, et al. Gene-specific countermeasures against Ebola virus based on antisense phosphorodiamidate morpholino oligomers. *PLoS Pathog*. 2006;2(1):e1. doi:10.1371/journal.ppat.0020001.
6. Hoffman EP, Brown RH Jr, Kunkel LM. Dystrophin: the protein product of the Duchenne muscular dystrophy locus. *Cell*. 1987;51(6):919-928.
7. Hoffman EP. Skipping toward personalized molecular medicine. *N Engl J Med*. 2007;357(26):2719-2722.
8. Dunckley MG, Villiet P, Eperon IC, Dickson G. Modification of splicing in the dystrophin gene in cultured *Mdx* muscle cells by antisense oligoribonucleotides. *Hum Mol Genet*. 1998;7(7):1083-1090.
9. van Deutekom JC, Janson AA, Ginjaar IB, et al. Local dystrophin restoration with antisense oligonucleotide PRO051. *N Engl J Med*. 2007;357(26):2677-2686.
10. Wheeler TM, Lueck JD, Swanson MS, Dirksen RT, Thornton CA. Correction of ClC-1 splicing eliminates chloride channelopathy and myotonia in mouse models of myotonic dystrophy. *J Clin Invest*. 2007;117(12):3952-3957.
11. Hua Y, Vickers TA, Baker BF, Bennett CF, Krainer AR. Enhancement of *SMN2* exon 7 inclusion by antisense oligonucleotides targeting the exon. *PLoS Biol*. 2007;5(4):e73. doi:10.1371/journal.pbio.0050073.
12. Asparuhova MB, Martí G, Liu S, Serhan F, Trono D, Schumperli D. Inhibition of HIV-1 multiplication by a modified U7 snRNA inducing Tat and Rev exon skipping. *J Gene Med*. 2007;9(5):323-334.
13. Kesari A, Pirra LN, Bremadesam L, et al. Integrated DNA, cDNA, and protein studies in Becker muscular dystrophy show high exception to the reading frame rule. *Hum Mutat*. 2008;29(5):728-737.
14. Yokota T, Duddy W, Partridge T. Optimizing exon skipping therapies for DMD. *Acta Myol*. 2007;26(3):179-184.
15. Covone AE, Lerone M, Romeo G. Genotype-phenotype correlation and germline mosaicism in DMD/BMD patients with deletions of the dystrophin gene. *Hum Genet*. 1991;87(3):353-360.
16. Talkop UA, Klaassen T, Plirsoo A, et al. Duchenne and Becker muscular dystrophies: an Estonian experience. *Brain Dev*. 1999;21(4):244-247.
17. Menhart N. Hybrid spectrin type repeats produced by exon-skipping in dystrophin. *Biochim Biophys Acta*. 2006;1764(6):993-999.
18. Béroud C, Tuffery-Giraud S, Matsuo M, et al. Multiexon skipping leading to an artificial DMD protein lacking amino acids from exons 45 through 55 could rescue up to 63% of patients with Duchenne muscular dystrophy. *Hum Mutat*. 2007; 28(2):196-202.
19. Nakamura A, Yoshida K, Fukushima K, et al. Follow-up of three patients with a large in-frame deletion of exons 45-55 in the Duchenne muscular dystrophy (*DMD*) gene. *J Clin Neurosci*. 2008;15(7):757-763.

Transduction Efficiency and Immune Response Associated With the Administration of AAV8 Vector Into Dog Skeletal Muscle

Sachiko Ohshima[1,2], Jin-Hong Shin[1,3], Katsutoshi Yuasa[1,4], Akiyo Nishiyama[1], Junichi Kira[2], Takashi Okada[1] and Shin'ichi Takeda[1]

[1]Department of Molecular Therapy, National Institute of Neuroscience, National Center of Neurology and Psychiatry, Tokyo, Japan; [2]Department of Neurology, Neurological Institute, Graduate School of Medical Sciences, Kyushu University, Fukuoka, Japan; [3]Department of Neurology, Graduate School of Medicine, Pusan National University, Busan, Republic of Korea; [4]Research Institute of Pharmaceutical Sciences, Faculty of Pharmacy, Musashino University, Tokyo, Japan

Recombinant adeno-associated virus (rAAV)-mediated gene transfer is an attractive approach to the treatment of Duchenne muscular dystrophy (DMD). We investigated the muscle transduction profiles and immune responses associated with the administration of rAAV2 and rAAV8 in normal and canine X-linked muscular dystrophy in Japan ($CXMD_J$) dogs. rAAV2 or rAAV8 encoding the *lacZ* gene was injected into the skeletal muscles of normal dogs. Two weeks after the injection, we detected a larger number of β-galactosidase-positive fibers in rAAV8-transduced canine skeletal muscle than in rAAV2-transduced muscle. Although immunohistochemical analysis using anti-CD4 and anti-CD8 antibodies revealed less T-cell response to rAAV8 than to rAAV2, β-galactosidase expression in rAAV8-injected muscle lasted for <4 weeks with intramuscular transduction. Canine bone marrow-derived dendritic cells (DCs) were activated by both rAAV2 and rAAV8, implying that innate immunity might be involved in both cases. Intravenous administration of rAAV8-*lacZ* into the hind limb in normal dogs and rAAV8-*microdystrophin* into the hind limb in $CXMD_J$ dogs resulted in improved transgene expression in the skeletal muscles lasting over a period of 8 weeks, but with a declining trend. The limb perfusion transduction protocol with adequate immune modulation would further enhance the rAAV8-mediated transduction strategy and lead to therapeutic benefits in DMD gene therapy.

Received 16 March 2008; accepted 17 September 2008; published online 21 October 2008. doi:10.1038/mt.2008.225

INTRODUCTION

Duchenne muscular dystrophy (DMD) is an inherited disorder causing progressive deterioration of skeletal and cardiac muscles because of mutations in the dystrophin gene. No effective treatment has been established despite the development of various novel therapeutic strategies including pharmacologic and gene therapies. Dystrophin-deficient *mdx* mice and dystrophin-utrophin double-knockout mice are the animal models most widely used to evaluate therapeutic efficacy, although the symptoms of *mdx* mice are not comparable to those of human DMD patients. Dystrophin-deficient canine X-linked muscular dystrophy was found in a golden retriever,[1,2] and we have established a Beagle-based model of canine X-linked muscular dystrophy in Japan ($CXMD_J$) dogs.[3] The clinical and pathological characteristics of the dystrophic dogs are more similar to those of DMD patients than murine models.[3]

The recombinant adeno-associated virus (rAAV) can be used for delivering genes to muscle fibers. Several serotypes of rAAV exhibit a tropism for striated muscles.[4,5] Intramuscular or intravenous administration of rAAV carrying the microdystrophin gene was reported to restore specific muscle force and extend the lifespan in dystrophic mice.[6,7] In contrast to the success of transgene delivery in mice, rAAV2 or rAAV6 delivery to canine striated muscles without immunosuppression resulted in insufficient transgene expression, and rAAV evoked strong immune responses.[8,9] An assay of interferon-γ released from murine and canine splenocytes suggested that the immune responses against rAAV and transgene products in mice and in dogs are dissimilar.[8] Uptake of rAAV2 by human dendritic cells (DCs) and T-cell activation in response to the AAV2 capsid have been reported,[10] indicating that DCs play key roles in the immune response against rAAV-mediated transduction. On the other hand, other serotypes, including rAAV8, that are capable of whole-body skeletal muscle expression after intravenous administration,[4,5] induce less T-cell activation.[11] We hypothesized that the level of activation of canine DCs by rAAV8 might be lower than that achieved by rAAV2. However, the transduction profile and immune response in the rAAV8-injected dog skeletal muscle have not been elucidated.

In this study, we chose to use intramuscular injections under ultrasonographic guidance so as to minimize the inflammatory reaction caused by incisional intramuscular injection.[8] In

Correspondence: Shin'ichi Takeda or Takashi Okada, Department of Molecular Therapy, National Institute of Neuroscience, National Center of Neurology and Psychiatry, 4-1-1 Ogawa-higashi, Kodaira, Tokyo 187-8502, Japan. E-mail: takeda@ncnp.go.jp or t-okada@ncnp.go.jp

addition, intravascular delivery was performed as a form of limb perfusion, in an attempt to bypass the immune activation of DCs in the injected muscle.[12] We investigated the transgene expression and host immune response to two distinct serotypes of rAAV in normal and dystrophic dogs after direct intramuscular injection and after limb perfusion.

RESULTS

Extensive expression of β-galactosidase in rAAV8-transduced muscles in wild-type dogs

We administered nonincisional intramuscular injections under ultrasonographic guidance so as to minimize injury. With incisional injection, the ordinary method of intramuscular viral administration in dogs,[8] the skin is opened to identify the individual muscles. This may enhance the immune reaction by recruiting inflammatory cells for wound healing. After nonincisional injection of rAAV2-*lacZ*, faint β-galactosidase (β-gal) expression was detected, whereas lymphocyte infiltration still occurred (**Supplementary Figure S1**). To investigate the transduction efficiency of rAAV8 in canine skeletal muscle, normal dogs were transduced with rAAV-*lacZ* serotypes 2 and 8 (**Table 1**). Prominent expression of β-gal was observed in the rAAV8-*lacZ*-injected muscles, whereas the rAAV2-*lacZ*-injected muscles showed minimal transgene expression (**Figure 1**). While β-gal expression in the rAAV8-injected muscle was correlated with the viral dose, β-gal expression in the rAAV2-injected muscle was not augmented with viral dose escalation. However, rAAV8-*lacZ*-injected muscles, which showed extensive β-gal expression at 2 weeks, also exhibited reduced expression at 4 weeks after the injection, thereby suggesting that the transgene product had immunogenicity (**Supplementary Figure S2**).

To evaluate the difference in transduction efficiency between rAAV2 and rAAV8 at 2 weeks after the injection, relative quantifications of the vector genome and mRNA were performed. The result demonstrated higher transduction rates in the rAAV8-injected muscles as increasing amounts of the vector were administered (**Figure 2a,b**). The amount of protein expression was also well correlated with that of transgenic DNA (**Figure 2c**, **Supplementary Table S1**). Immunohistochemical analysis revealed that the rAAV2-injected muscles showed much more infiltration of $CD4^+$ and $CD8^+$ T lymphocytes in the endomysial space than the rAAV8-injected muscles did (**Figure 3a**). mRNA levels of TGF-β1 and IL-6 (representative markers of inflammation) in the rAAV-injected muscles were standardized with the β-gal expression. rAAV2-injected muscles had higher TGF-β1 and IL-6 expression than rAAV8-transduced muscles (**Supplementary Figure S3**). We also examined humoral immune responses against the rAAV particles in the sera of rAAV-injected dogs. The levels of serum IgG in reaction to rAAV2 or rAAV8 gradually increased with time in both serotypes (**Figure 3b**). These results suggest

Table 1 Summary of gene transduction experiments

Dog ID	Sex	Age[a]	BW[b]	rAAV serotype	Transgene	Route	Muscle	Vector dose[c]	Transgene expression[d]			Cellular infiltration[e]		
									2 weeks	4 weeks	8 weeks	2 weeks	4 weeks	8 weeks
2201MN	M	10	4.5	2	lacZ	i.m.	TA, ECR	1×10^{11}	−	−		−	++	
3004MN	M	5	2.8	2	lacZ	i.m.	TA, ECR	1×10^{11}	±	−		+	±	
3007FN	F	5	2.5	2	lacZ	i.m.	TA, ECR	1×10^{11}	±	±		++	++	
2204FN	F	10	2.5	2	lacZ	i.m.	TA, ECR	1×10^{12}	−	−		+	++	
2801FN	F	10	5.2	2	lacZ	i.m.	TA, ECR	1×10^{12}	+	−		+	++	
2901MN	M	6	2.8	2	lacZ	i.m.	TA, ECR	1×10^{12}	−			±		
7M48	M	7	3.3	2	lacZ	i.m.	TA, ECR	1×10^{12}	−			+		
2206FN	F	10	3.0	2	lacZ	i.m.	TA, ECR	1×10^{13}	±	±		+	++	
2205MN	M	10	4.2	8	lacZ	i.m.	TA, ECR	1×10^{11}	++	±		−	++	
2905MN	M	6	2.8	8	lacZ	i.m.	TA, ECR	1×10^{11}	±			−		
NL52F	F	10	3.5	8	lacZ	i.m.	TA, ECR	1×10^{12}	+++			±		
2106FN	F	6	3.2	8	lacZ	i.m.	TA, ECR	1×10^{12}	+++	−		−	++	
7M49	F	6	3.2	8	lacZ	i.m.	TA, ECR	1×10^{12}		±	−		++	±
2109FMN	M	7	3.3	8	lacZ	i.m.	TA, ECR	1×10^{12}	+++			−		
2903MN	M	6	3.2	8	lacZ	i.m.	TA, ECR	1×10^{12}	+++			±		
2209MN	M	10	4.3	8	lacZ	i.m.	TA, ECR	1×10^{13}	+++	±		±	+++	
2309FA	F	6	3.2	8	M3	i.m.	TA, ECR	1×10^{12}	±	+				
LH49F	F	8	3.3	8	lacZ	i.v.		1×10^{14}	+++			+		
3805MN	M	6	3.5	8	lacZ	i.v.		1×10^{14}		+++	+		+	+
2704FA	F	8	3.6	8	M3	i.v.		1×10^{14}	+	+++				
4001MA	M	6	3.2	8	M3	i.v.		1×10^{14}		+++	+			

BW, body weight; F, female; M, male.
[a]Age at injection (weeks). [b]BW at injection (kg). [c]Vectors (vg/ml) were intramuscularly (i.m.) injected into extensor carpi radiolis (ECR) (1 ml) and tibialis anterior (TA) (2 ml) on both sides. Vectors were also intravenously (i.v.) injected into the lateral saphenous vein (vg/kg/limb) by using limb perfusion method. [d]β-Gal or microdystrophin-positive fibers per 3,000 fibers: −, 0; ±, <100; +, <300; ++, <1,000; +++, >1,000. [e]Infiltrating cells: −, not detected; ±, a few; +, moderate; ++, extensive.

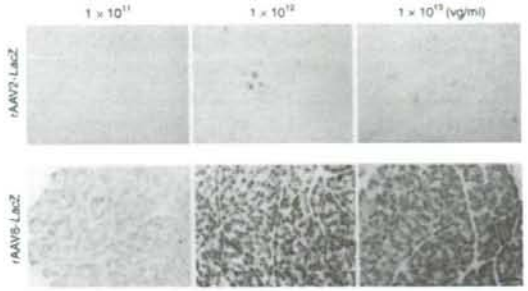

Figure 1 Canine skeletal muscles stained for β-galactosidase. Two milliliters of rAAV2-*lacZ* or rAAV8-*lacZ* (1×10^{11}–10^{13} vg/ml) were injected intramuscularly into the tibialis anterior (TA) muscle of normal dogs ($n = 16$) under ultrasonographic guidance. The muscles were biopsied 2 weeks after the injection. Upper: rAAV2-*lacZ*-injected TA muscles, Lower: rAAV8-*lacZ*-injected TA muscles. Bar = 200 μm.

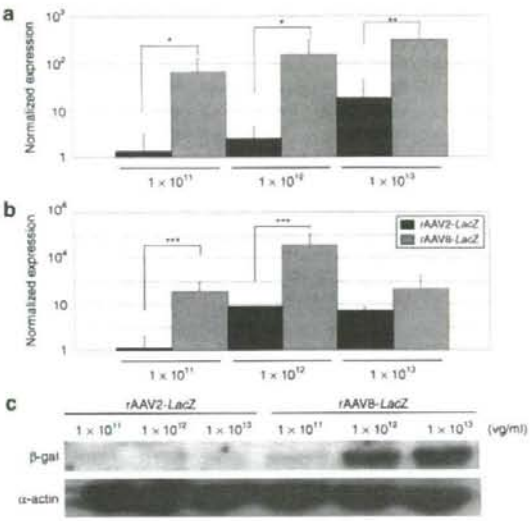

Figure 2 Quantification of viral vector genome, mRNA, and transgene expression. (a) Relative quantification of genomic PCR for rAAV2-*lacZ*-injected muscle (black bars) or rAAV8-*lacZ*-injected muscle (gray bars). DNA samples were extracted from the TA muscles. $^{*}P < 0.05$. $^{**}P < 0.01$. Error bars represent 2 SD. **(b)** Relative quantification showed more extensive β-gal mRNA expression caused by rAAV8-*lacZ* (gray bars) as compared to that caused by rAAV2-*lacZ* (black bars). 18S rRNA was used for an internal control. $^{***}P < 0.05$. Error bars represent 2 SD. **(c)** Western blots of β-gal protein (120 kDa) and α-actin (42 kDa); the β-gal signal was normalized to α-actin for comparison.

that cellular and humoral immune responses are elicited in both rAAV2- and rAAV8-transduced muscles.

Bone marrow-derived DC reactions to rAAV2 and rAAV8

We next cultured bone marrow-derived DCs to investigate their response to rAAV injection in dogs. Flow cytometric analyses of these cells at 7 days of culture revealed marked expressions of CD11c and MHC class II molecules on the

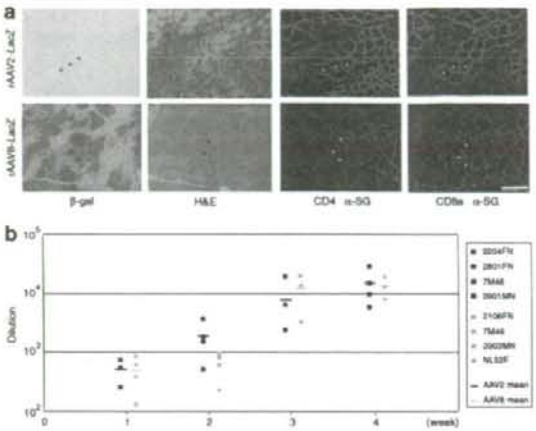

Figure 3 Immune response to rAAV. (a) Lymphocyte infiltration after rAAV transduction. Muscles were biopsied 2 weeks after rAAV2- or rAAV8-*lacZ* injection (2×10^{12} vg/muscle). Serial cross-sections were stained with β-gal and H&E, and were immunohistochemically stained with antibodies against canine CD4, CD8a (Alexa 568, red), and α-sarcoglycan (α-SG, Alexa 488, green). Upper: rAAV2-*lacZ*-injected TA muscle; lower: rAAV8-*lacZ*-injected TA muscle. Bar = 100 μm. **(b)** Humoral immune responses to rAAV capsid in dogs. Serum was collected weekly from rAAV2- or rAAV8-*lacZ*-injected dogs and analyzed for the presence of IgG antibody against the rAAV2 or rAAV8 capsid. The data represent dilution rates with 50% reactivity of anti-rAAV2 (black boxes) and anti-rAAV8 (gray boxes) capsid antibodies. The mean reconstitution values are shown as straight lines. Each symbol represents an individual dog that was injected with rAAV at 2×10^{12} vg/muscle.

surface (**Figure 4a,b**). The DCs were cultured with the rAAV-*luciferase* of either serotype 2 or 8 for 48 hours to evaluate transduction efficiency, or cultured with rAAV-*lacZ* for 4 hours to investigate kinetic changes in mRNA. The luciferase assay showed that the transduction efficiency of rAAV2-*luciferase* in DCs was approximately two times that of rAAV8-*luciferase* (**Figure 4c**). mRNA levels of MyD88 and costimulating factors, such as CD80, CD86, and type I interferon (interferon-β, IFN-β) were elevated in both conditions (**Figure 4d**), suggesting that rAAV8 also induces a considerable degree of innate immune response in dog skeletal muscles. Although rAAV2-transduced DCs showed higher IFN-β expression than rAAV8-transduced DCs, the differences between the effects of rAAV2 and rAAV8 on the mRNA levels of MyD88, CD80, CD86, and IFN-β were not statistically significant.

Successful *microdystrophin* gene transfer with rAAV8 into dystrophic dogs

Dystrophin expression in normal skeletal muscle is localized on the sarcolemma, whereas it is totally absent in $CXMD_J$ dogs (**Supplementary Figure S4a,b**). Microdystrophin expression in the rAAV8-injected skeletal muscle of $CXMD_J$ dogs was maintained, even in the absence of any immunosuppressive therapy, for at least 4 weeks after the injection (**Table 1**). Previously, we had shown that microdystrophin expression of ca 20% was sufficient to achieve functional recovery in mdx mice[6]. However, the amount of the expression in intramuscularly injected muscles

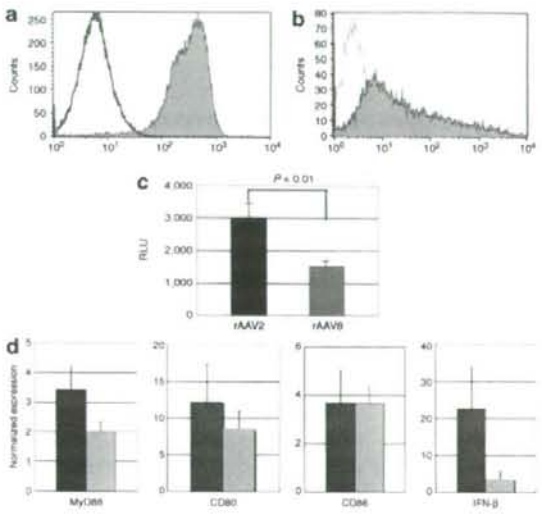

Figure 4 Responses of dendritic cells (DCs) to rAAV in dogs. Bone marrow-derived DCs were obtained from the humerus bones of dogs and cultured in RPMI (10% FCS, p/s) for 7 days with canine GM-CSF and IL-4. (**a**) Flow cytometric analysis of cell surface molecules on day 7. The cells were stained with PE-conjugated CD11c antibody and isotype control. (**b**) DCs were stained with FITC-conjugated MHC Class II antibody and isotype control. (**c**) DCs were transduced with rAAV-*luciferase* (1×10^6 vg/cell) for 48 hours. To analyze luciferase expression relating to the use of rAAV2 or rAAV8, relative light unit (RLU) ratios were measured. $^*P < 0.01$. Error bars represent s.e.m., $n = 8$. (**d**) DCs were transduced with 1×10^6 vg/cell of rAAV2 (black bars) or rAAV8-*lacZ* (gray bars) for 4 hours, and mRNA levels of MyD88, CD80, CD86, and IFN-β were analyzed. Untransduced cells were used as a control to demonstrate the relative value of expression. The results are representative of two independent experiments. Error bars represent s.e.m., $n = 3$.

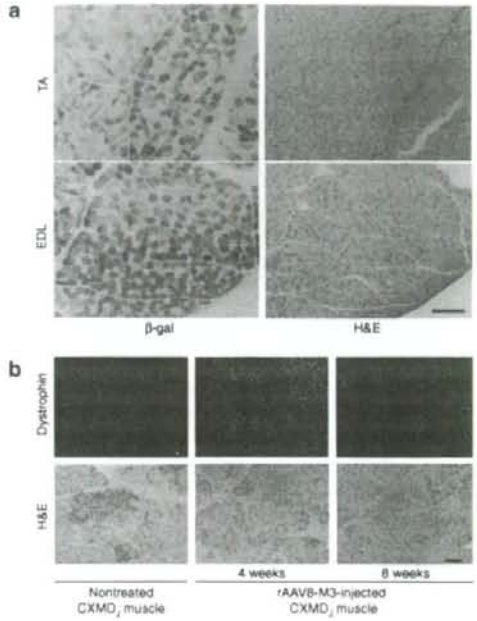

Figure 5 rAAV8-mediated muscle transduction using the limb perfusion method. (**a**) Transduction of normal dog with rAAV8-*lacZ*, using the limb perfusion method. Muscles were biopsied 2 weeks after the injection and stained with β-gal and H&E. TA, tibialis anterior, EDL, extensor digitorum longus. Bar = 200 μm. (**b**) Transduction of canine X-linked muscular dystrophy in Japan (CXMD$_j$) dog with rAAV8-*M3*. Muscles of CXMD$_j$ dogs were biopsied 4 and 8 weeks after limb perfusion with rAAV8-*M3*. Samples were immunohistochemically stained with anti-dystrophin antibody (dys2, NCL). Left: nontreated CXMD$_j$ muscle. Middle and right: muscles injected with rAAV-*M3* using limb perfusion method, examined at 4 or 8 weeks after the transduction. Bar = 100 μm.

seemed to be insufficient to produce the expected functional recovery (**Supplementary Figure S4c**).

For more efficient gene delivery by rAAV8, we tried a limb perfusion method in the hind limb through the lateral saphenous vein, in an attempt to prevent muscle damage due to direct injection and to bypass immune activation through DCs in the injected muscle. We had observed highly efficient β-gal expression in nearly all the muscles of the distal hind limb at 2 weeks after a single injection (**Table 1**, **Figure 5a**). We then injected rAAV8-*M3* into the hind limbs of CXMD$_j$ dogs, using the same method (**Table 1**). The induction of microdystrophin expression in the muscle at 4 weeks after intravascular injection was more efficient and free of noticeable immune response as compared to intramuscularly injected muscle (**Figure 5b**, **Supplementary Figure S4d**). These results suggest that the intravascular method is superior to the intramuscular method of administration. Although microdystrophin expression persisted at 8 weeks after injection of rAAV8-*M3*, the number of microdystrophin-positive cells at this time point was lower than in the muscles that were sampled at 4 weeks after injection. It is clear, therefore, that long-term microdystrophin expression can be obtained by the limb perfusion method, but that the expression does not last at the same level over a period of weeks. The same phenomenon was observed in rAAV8-*lacZ*-transduced muscles (**Supplementary Figure S5**).

DISCUSSION

In this article, we present evidence that the transfer of rAAV8-*lacZ* to canine skeletal muscles produces higher transgene expression with less lymphocyte proliferation than rAAV2-*lacZ* does, at 2 weeks after injection. Given the advantages of rAAV8, the administration of rAAV8-*M3* by limb perfusion produced extensive transgene expression in the distal limb muscles of CXMD$_j$ dogs without obvious immune responses for as long as 8 weeks after injection. However, transgene expression in the rAAV8-transduced muscles attenuated in the absence of an immunosuppressive regimen over the course of observation. In addition, humoral immune responses were elicited by both rAAV2 and rAAV8. mRNA levels of MyD88 and costimulating factors such as CD80, CD86, and type I interferon (interferon-β) were elevated in both rAAV2- and rAAV8-transduced DCs *in vitro*.

In our previous study, we had demonstrated extensive lymphocyte-mediated immune responses to rAAV2-*lacZ* after direct intramuscular injection into dogs, in contrast to the reported successful delivery of the same viral construct into mouse skeletal

muscle.[8] The fact that the promoter-deleted rAAV2 caused fewer cytotoxic cellular responses suggested that the massive destruction of transduced muscle cells might be the result of cellular immunity against the transgene product. In this study, there was extensive expression of β-gal in rAAV8-*lacZ*-injected canine muscles even in the absence of any immunosuppressive treatments (**Figure 1**), while the rAAV2-*lacZ*-injected muscles showed minimal β-gal expression with considerable inflammatory infiltration. If the transgene product were the main inducer of immune responses, lymphocyte activation would be correlated with transduction efficiency; however, this is not the case based on our results relating to the vector genome, mRNA expression level, and protein delivered through either rAAV2 or rAAV8 (**Figure 2**). These data suggested that the rAAV particle is associated with potent immunogenicity. Besides, β-gal expression disappeared 4 weeks after injection in the rAAV8-injected muscle as in the rAAV2-transduced muscles (**Supplementary Figure S2**). To investigate whether AAV itself has immunogenicity properties, we further characterized the immune responses caused by rAAV2 or rAAV8.

Immunohistochemical analysis revealed that the rAAV2-injected muscles showed higher rates of infiltration of $CD4^+$ and $CD8^+$ T lymphocytes in the endomysium than rAAV8-injected muscles did (**Figure 3a**). Considering the stringent immunogenicity of *lacZ* gene expression, we normalized the activity of TGF-β1 and IL-6 by lacZ expression to exclude the effect of transgene products (**Supplementary Figure S3a**). The total activity of TGF-β1 and IL-6 in the rAAV8-injected muscles was higher than that in rAAV2-injected muscles (**Supplementary Figure S3b**). As a result, rAAV2 induced a stronger cellular immune response than rAAV8 did. To investigate the humoral immune response, we quantitated neutralizing antibodies against rAAV particles in the sera of rAAV-injected dogs (**Figure 3b**). Antibodies against AAV2 and AAV8 capsids were below the detectable level before the injection and were elevated with time after the injection. Because the dogs were bred in a specific pathogen-free facility and not vaccinated, we assume that the elevation of antibody levels was not caused by anamnestic reaction.

Recently, Li *et al.*[10] reported that the AAV2 capsid can induce a cellular immune response through MHC class I antigen presentation with a cross-presentation pathway, and the effects of rAAV2 on human DCs have been described.[10,13] In contrast, other serotypes such as rAAV8 induced less T-cell activation.[11,14] Plasmacytoid DCs are critically important in innate immunity because of their unsurpassed ability to present adenoviral antigens to T-cells for the generation of primary cellular and humoral immune responses.[15–17] The response of DCs against rAAV in dogs was yet to be elucidated. We prepared bone marrow-derived DCs to investigate rAAV-mediated transduction of DCs. The difference between rAAV2 and rAAV8 in respect of the transduction rate of DCs *in vitro* was no greater than the difference in distinct β-gal expressions *in vivo* (**Figure 2,4c**). Quantitative analysis of mRNA of the transduced DCs by RT-PCR revealed that both rAAV2 and rAAV8 upregulated the expression of costimulating factors, with no significant difference between mRNA levels in rAAV2- and rAAV8-transduced cells. Therefore, both rAAV2 and rAAV8 may activate innate immunity in the context of extensive muscle transduction. Whereas AAV capsids cause immune response, transgene products may play adjuvant roles in the immunity to the AAV capsids.[18]

rAAV8 encoding the human *microdystrophin* gene was also intramuscularly injected into the skeletal muscles of $CXMD_J$ dogs. rAAV8-mediated gene expression without any immunosuppression was confirmed over a period of 8 weeks after the injection, whereas there was much less transduction with the use of rAAV2 (data not shown). rAAV8-mediated transduction was also expected to provide effective intravenous delivery.[12] In this context, the venous system is an attractive route for limb perfusion administration because it is a direct channel to multiple muscles of the limb. Moreover, veins are easier to access through the skin and there is less potential for muscle damage during injection. By using the limb perfusion method, we could reach nearly all the muscles of the lower limb, held transiently isolated by a tourniquet around the thigh. Limb perfusion administration could possibly have the potential to bypass the DC recognition caused by intramuscular injection. We intravenously injected rAAV8-*lacZ* into the hind limbs of normal dogs and rAAV8-*M3* into the hind limbs of $CXMD_J$ dogs, and obtained more extensive expression of β-gal or microdystrophin than by intramuscular injection. Interestingly, the inflammatory response was not significant in the intravenously injected muscles, although no immune suppression was attempted. We think that one reason rAAV8-*M3* resulted in better expression than rAAV8-*lacZ* is that the immunogenicity of *M3* is lower than that of *lacZ*. Although microdystrophin expression was lower at 8 weeks after the transduction with the limb perfusion, cellular infiltration was not significant.

In the future, systemic delivery of rAAV8-*microdystrophin* could ameliorate the symptoms of DMD patients. Even though portal vein injection of rAAV2-*FIX* into hemophilia B dogs produced long-term expression, a clinical study failed to demonstrate long-term expression in humans.[19,20] In advance of future clinical trials, several studies are required to confirm safety. Sequential peripheral blood monitoring showed no severe adverse events, including liver dysfunction, during 8 weeks (data not shown). We are now developing a systemic delivery strategy with a muscle-specific promoter. It is also necessary to improve vector constructs or regulate immune reaction against transgene products. Recently, Wang *et al.* reported sustained AAV6-mediated human microdystrophin expression in dystrophic dogs for 30 weeks, using combined immunosuppressive therapy of Ciclosporin, Mycophenolate Mofetil, and anti-thymocyte globulin.[9] In this study with rAAV8-*M3*, we confirmed effective transduction into dog skeletal muscle for 4 weeks without immunosuppressive therapy. However, considering the fact that not only rAAV2 but also rAAV8 induced activation of DCs *in vitro*, immunological modulation would be required for sufficient long-term expression. A novel protocol with systemic or localized immunosuppression using immunosuppressive drugs or local immunosuppression with an IFN-α or -β blockade could help avoid host immune reaction.

In summary, we achieved successful rAAV8-mediated muscle transduction in wild-type dogs as well as in dystrophic dogs by using the limb perfusion method of administration. Also, by manipulating bone marrow-derived DCs, we observed the probable contribution of antigen-presenting cells to the immune response against rAAV8-mediated gene therapy. Although the

cellular responses against rAAV8 were not significant *in vivo*, this DC activation may possibly be involved in limiting long-term transduction when the limb perfusion method is used. The limb perfusion transduction protocol with improved AAV constructs or immune modulation would further enhance rAAV8-mediated transduction strategy and lead to therapeutic benefits.

MATERIALS AND METHODS

Animals. Five- to ten-week-old male and female wild-type dogs obtained from the Beagle-based $CXMD_j$ breeding colony at the National Center of Neurology and Psychiatry (Tokyo, Japan) were used for the *lacZ* gene transduction.[3] Six- to eight-week-old $CXMD_j$ dogs were used for *microdystrophin* gene transduction. All the animals were cared for and treated in accordance with the guidelines approved by the Ethics Committee for Treatment of Laboratory Animals at National Center of Neurology and Psychiatry, where the three fundamental principles of replacement, reduction, and refinement are also considered. Dogs were not vaccinated to avoid the immune responses to vaccination.

Construction of proviral plasmid and recombinant AAV vector production. The AAV2 vector proviral plasmids harboring the *lacZ* or *luciferase* gene with a CMV promoter and SV40 late-gene polyadenylation sequence were propagated.[8] As a therapeutic gene for DMD, the human *microdystrophin* gene, *M3*, was used under the control of the CMV promoter and a bovine growth hormone polyadenylation sequence.[21] The vector genome was packaged into the AAV2 capsid or pseudotyped AAV8 capsid in HEK293 cells. A large-scale cell culture method with an active gassing system was used for transfection.[22] The vector production process involved triple transfection of a proviral plasmid, an AAV helper plasmid pAAV-RC (Stratagene, La Jolla, CA) or p5E18-VD2/8, and an adenovirus helper plasmid pHelper (Stratagene).[21] All the viral particles were purified by CsCl gradient centrifugation. The viral titers were determined by quantitative PCR using SYBR-green detection of PCR products in real time with the MyiQ single-color detection system (Bio-Rad, Hercules, CA) and the following primer sets: for AAV-*lacZ*, lacZ-Q60: forward primer 5′-TTATCAGCCGGAAAACCTACCG-3′, and reverse primer 5′-AGCCAGTTTACCCGCTCTGCTA-3′; for AAV-*microdystrophin*: forward primer 5′-CCAAAAGAAAAAGGATCCACAA-3′, and reverse primer 5′-TTCCAAATCAAACCAAGAGTCA-3′; and for AAV-*luciferase*: forward primer 5′-GATACGCTGCTTTAATGCCTTT-3′, and reverse primer 5′-GTTGCGTCAGCAAACACAGT-3′.

Direct administration of rAAVs into normal and dystrophic skeletal muscle. Experimental dogs ($n = 16$) were sedated with isoflurane by mask inhalation and intubated. Anesthesia was maintained with 2–4% isoflurane. Two milliliters of rAAV2-*lacZ* or rAAV8-*lacZ* (1×10^{11}–10^{13} vg/ml) were injected intramuscularly into the tibialis anterior muscles and 1 ml into the extensor carpi radialis muscles of the normal dogs under ultrasonographic guidance. rAAV8-*M3* (1×10^{12} vg/ml) was intramuscularly injected at a volume of 2 ml into the tibialis anterior muscles and 1 ml into the extensor carpi radialis muscles of a $CXMD_j$ dog.

Intravenous delivery of rAAVs into the limb veins of dogs. Intravenous injection was administered as described elsewhere.[12] Briefly, a blood pressure cuff was applied just above the knee of an anesthetized normal dog. A 24-gauge intravenous catheter was inserted into the lateral saphenous vein, connected to a three-way stopcock, and flushed with saline. With the blood pressure cuff inflated to over 300 mm Hg, saline (2.6 ml/kg) containing papaverine (0.44 mg/kg, Sigma-Aldrich, St Louis, MO) and heparin (16 U/kg) was injected by hand over 10 seconds. The three-way stopcock was connected to a syringe containing rAAV8-*lacZ* (1×10^{14} vg/kg, 3.8 ml/kg). The syringe was placed in a PHD 2000 syringe pump (Harvard Apparatus, Edenbridge, UK). Five minutes after the papaverine/heparin injection, the rAAV8-*lacZ* was injected at a rate of 0.6 ml/second. Two minutes after the rAAV injection, the blood pressure cuff was released and the catheter was removed. The $CXMD_j$ dogs were injected with rAAV8-*M3* using the same method.

Sampling of transduced muscles. Either the muscles of the transduced dogs were biopsied or the animals were killed at 2, 4, and 8 weeks after the injection. We sampled tibialis anterior and extensor carpi radialis muscles on both sides in the intramusculary transduced dog. In the case of the limb perfusion study, tibialis anterior or extensor digitorum longus muscle of the injected side of the leg was sampled. For biopsy and necropsy, the individual muscle was cropped tendon-to-tendon, divided into several pieces, and immediately frozen in liquid nitrogen-cooled isopentane. Two to eight blocks were sampled from the transduced muscle. We analyzed at least 30 sections from the blocks to observe the general representation.

Histological analysis. Transverse cryosections (10 μm) from the rAAV-*lacZ*-injected muscles were stained with hematoxylin and eosin or 5-bromo-4-chloro-3-indolyl-β-D-galactopyranoside.[23] Eight-micrometer-thick cryosections from the rAAV-*M3*-injected muscles were immunohistochemically stained as described.[24] Briefly, the cryosections were fixed by immersion in cold acetone at −20 °C. Fixed frozen sections were blocked in 5% goat serum in phosphate-buffered saline at room temperature and incubated with mouse monoclonal anti-dystrophin C-terminal antibody (NCL-dys2, Novocastra, Newcastle upon Tyne, UK). The signal was visualized with an Alexa 568-conjugated anti-mouse IgG. Fluorescent signals were observed using a confocal laser scanning microscope (Leica TCS SP, Leica, Heidelberg, Germany). Immunohistochemical analyses were performed with mouse monoclonal antibodies against canine CD4 (CA13.1E4, Serotec, Oxford, UK), canine CD8a (CA9. JD3, Serotec), and double-stained with rabbit polyclonal antibody against α-sarcoglycan.[25] The signal was visualized with an Alexa 568-conjugated anti-mouse IgG, and 488-conjugated anti-rabbit IgG.

Detection of AAV genomes. Total DNA was extracted from muscle cryosections. Cryosections were homogenized using a Multi-beads shocker (Yasui Kikai, Osaka, Japan), and extracted using a Wizard SV Genomic DNA purification system (Promega, Madison, WI). The rAAV genome was detected by relative quantitative PCR using SYBR-green detection of PCR products in real time with a primer set of *lacZ*-Q60. For an internal control, forward primer, 5′-GAACACGCGTTAATAAGGCAATCA-3′, and reverse primer, 5′-CTGACATTCATCGCATCTTTGACA-3′, directed to an ultra-conserved region, were used.[26]

Real-time RT-PCR. Total RNA was isolated from cryosections using a Multi-beads shocker (Yasui Kikai), and RNeasy Fibrous Tissue Mini kit (Qiagen, Hilden, Germany), and first-strand cDNA was synthesized using a QuantiTect Reverse Transcription kit (Qiagen). mRNA was detected using primer sets of lacZ-Q60, forward primer 5′-TGATGGCTA CTGCTTTCCCTAC-3′ and reverse primer 5′-GAGATTTTGCCGA GGATGTACT-3′ for IL-6, and forward primer 5′-CAAGGATCTGGGC TGGAAGTGGA-3′ and reverse primer, 5′-CCAGGACCTTGCTGTA CTGCGGT-3′ for TGF-β1. For an internal control, a primer set of 18S rRNA (Ambion, Foster City, CA) was used.

Western blot analysis. Muscle cryosections were homogenized with four volumes of sample buffer (10% SDS, 70 mmol/l Tris-HCl, 10 mmol/l EDTA, and 5% β-mercaptoethanol). The samples were boiled for 5 minutes and centrifuged at 14,500 rpm for 15 minutes. Protein samples (30 μg per lane) were electrophoresed on a 7.5% polyacrylamide gel (Bio-Rad). The membranes were incubated with a 1:1,000 dilution of the primary antibody for detecting 120 kDa lacZ protein (rabbit anti-β-galactosidase IgG fraction, Molecular Probes, Eugene, OR) or 42 kDa α-actin (mouse anti α-sarcomeric actin IgM, Sigma-Aldrich). Anti-rabbit IgG peroxidase F(ab′)